NASA CONTRACTOR REPORT

NASA CR-2542

4.
EVALUATION OF A SERIES HYBRID THRUST BEARING AT DN VALUES TO THREE MILLION (FINAL REPORT)

II - Fabrication and Testing

M. Eusepi and L. W. Winn

Prepared by
3.
MECHANICAL TECHNOLOGY INCORPORATED
Latham, N.Y. 12110
for Lewis Research Center

NATIONAL AERONAUTICS AND SPACE ADMINISTRATION • WASHINGTON, D. C. • JUNE 1975

1. Report No.	2. Government Accession No.	3. Recipient's Catalog No.
NASA CR-2542		

4. Title and Subtitle	5. Report Date
EVALUATION OF A SERIES HYBRID THRUST BEARING AT DN VALUES TO THREE MILLION II - FABRICATION AND TESTING	June 1975 6. Performing Organization Code
7. Author(s) M. Eusepi and L. W. Winn	8. Performing Organization Report No. MTI 75TR19
9. Performing Organization Name and Address Mechanical Technology Incorporated 968 Albany-Shaker Road Latham, New York 12110	10. Work Unit No. 11. Contract or Grant No. NAS 3-16740
12. Sponsoring Agency Name and Address National Aeronautics and Space Administration Washington, D.C. 20546	13. Type of Report and Period Covered Contractor Report 14. Sponsoring Agency Code

15. Supplementary Notes

Final Report. Project Manager, Herbert W. Scibbe, Fluid System Components Division, NASA Lewis Research Center, Cleveland, Ohio

16. Abstract

This report provides results of tests to determine the experimental performance of a series hybrid bearing. The bearing consists of a 150 mm ball bearing and a centrifugally actuated, conical, fluid-film bearing fitting an envelope with an outer radius of 86.4 mm (3.4 in.) and an inner radius of 71 mm (2.8 in.). Tests were conducted up to 16,500 rpm, at which speed an axial load of 15,568 N (3500 lb) was safely supported by the hybrid bearing system. Through the employment of the series hybrid bearing principle, it was possible to reduce the effective ball bearing speed to approximately one-half of the shaft speed. A reduction of this magnitude should result in a tenfold increase in the ball bearing fatigue life. A successful simulation of fluid-film bearing lubricant supply failure, performed repeatedly at an operating speed of 10,000 rpm, resulted in complete and smooth change-over to full-scale ball bearing operation when the oil supply to the fluid-film bearing was discontinued. Reactivation of the fluid-film supply system produced a flawless return to the original mode of hybrid operation.

17. Key Words (Suggested by Author(s))	18. Distribution Statement
Bearings; Ball bearings; Conical hydrostatic bearings; Hybrid thrust bearings	Unclassified - unlimited STAR Category 37 (rev.)

19. Security Classif. (of this report)	20. Security Classif. (of this page)	21. No. of Pages	22. Price*
Unclassified	Unclassified	45	$3.75

* For sale by the National Technical Information Service, Springfield, Virginia 22151

TABLE OF CONTENTS

LIST OF FIGURES

LIST OF TABLES

SUMMARY

The objective of this work was to test a series hybrid bearing applicable to advanced jet engine systems. The hybrid bearing configuration consists of a series combination of a conical, fluid-film bearing and a 150 mm ball bearing. The fluid-film bearing is unique in the sense that it takes advantage of centrifugal inertia forces, established by rotor rotation, to develop hydrostatic lubricant pressures. The pressurized lubricant is fed to orifices which terminate in pockets at the bearing interface. The pockets are equally spaced with a depth designed so as to yield orifice compensation over the operating range of film thickness.

The experimental performance of the series hybrid bearing, as provided by this report, has proven the series hybrid principle to be a viable means of reducing DN levels of large ball bearings operating in high-speed, high load systems. The tests were conducted up to 16,500 rpm at which time an axial load of 3,500 lbs. was safely supported by the series bearing system. The 16,500 rpm speed combined with the ball bearing diameter of 150 mm yields an operating value of 2.5 million DN. Through the employment of the series hybrid bearing principle, it was possible to reduce the effective bearing speed to approximately one-half of the shaft speed. A reduction of this magnitude could easily result in a ball bearing fatigue life increase by an order of magnitude.

Because of inherent limitations in the capacity of the oil system employed in this series of tests, the speed of 20,000 rpm equivalent to a DN value of 3 million could not be reached. Separate fluid-film bearing tests performed with hydraulically supplied pressures do indicate, however, that loads of 4,000 lbs. can be safely sustained at equivalent DN values of 20,000 rpm.

A successful simulation of lubricant supply failure to the fluid-film bearing performed as the unit was operating at 10,000 rpm, indicated that the series hybrid bearing possesses the inherent capability of affecting a complete and smooth change-over to full scale ball bearing operation when the oil supply to the fluid-film bearing is discontinued.

The combination of the effective speed-reducing action and demonstrable fail-safe features should place the series hybrid bearing concept as a prime contender for high-speed, high load applications which impose severe reductions on ball bearing fatigue life.

I. INTRODUCTION

An important consideration in the application of ball bearings to larger, high-speed rotating machinery is the improvement of fatigue life. Attempts to increase fatigue life by reducing the mass of rotating parts including the use of low mass hollow or drilled balls and rollers, have been demonstrated with limited success at the Lewis Research Center. Another method for improving fatigue life of a ball bearing is to reduce its rotational speed by coupling it in series with a fluid-film bearing. This arrangement is called the series hybrid bearing. In the series hybrid bearing, each bearing carries the full thrust load, but at partial speed. The inner fluid-film bearing member rotates with the shaft at full speed. The mating fluid-film bearing member rotates with the ball bearing inner race at some fraction of the shaft speed. The outer race of the ball bearing is mounted in a stationary housing. As shaft speed increases, the fluid-film bearing lifts due to the hydrostatic pressure developed by the centrifugal force of the lubricant fed through the shaft. At lift off, a speed differential between the inner member of the fluid-film bearing and intermediate member attached to the inner race of the ball bearing develops. This speed differential produces a lower speed for the ball bearing and thereby reduces ball centrifugal force (and thus contact stress) at the outer race. Reductions in ball bearing inner race speeds up to 33 percent have been successfully demonstrated in a test program at Lewis Research Center, (Reference 1).

The series hybrid bearing has several advantages when compared to both the hollow and drilled ball bearing concepts at DN (bearing bore in mm times shaft speed in rpm) values from 3 to 4 million. The most important of these advantages is the substantial improvement in bearing life obtained with a conventional ball bearing. Furthermore, the built-in fail-safe features provided by the ball bearing, make the series hybrid bearing a very attractive high-speed bearing concept.

The analytical and design phase of this program was summarized in "Evaluation of a Series Hybrid Bearing at DN Value to Three Million," I - Analysis and Design, NASA CR-2366, January 1974.

This report describes the fabrication, and testing of a series hybrid bearing configuration over a range of preselected running conditions. A conical hydrostatic fluid-film bearing coupled to a 150 mm bore angular contact, split-inner ring ball bearing is specified for the series hybrid bearing configuration. The fluid-film bearing is optimally designed with a low torque-rotational speed characteristic, matching that of the ball bearing at high rotative speeds.

II. TEST VEHICLE DESCRIPTION

The test rig design evaluation from which the actual test rig hardware evolved was presented in Reference [2] and will not be repeated here. The description of the actual hybrid tester, however, will be repeated in this report to maintain continuity.

A. Machine Parts

The major components of the series hybrid bearing test vehicle consist of parts illustrated in Figure 1. These parts are identified as follows: A conical fluid-film bearing runner (1) provided with drilled passages for lubricant supply is firmly shrunk onto a high-speed spindle shaft (2) (formerly employed in a NASA program described in Reference 1) and is additionally clamped in position by a retaining nut (3). The mating portion of the fluid-film bearing, referred to as the intermediate bearing member (4) includes the seat for the split inner race of the ball bearing (5) and the bearing retainer ring (4a). The outer race ball bearing is mounted in the test bearing housing (6). The remaining test head parts consist of the end cover (7), a position sensor mounting ring (8), and a seal plate (9). Lubricant supply to both the fluid-film and the ball bearing is provided by two long jet supply tubes (10), which penetrate the end cover (7) through liquid tight fittings. These tubes are positioned at the inner diameter of the intermediate member (4). Oil entering the receiving groove is then centrifugally pumped through drilled passages to the lubricating channels incorporated in the ball bearing's inner race. Fluid-film lubrication is supplied by a feed tube (11), which is securely attached to the end cover (7) and penetrates the hollow spindle shaft (2) far enough to reach an area between two oil baffles (12). Oil exiting the feed tube is centrifugally pumped through drilled passages in both the spindle shaft (2) and the fluid-film bearing runner (1) to the bearing interface. Oil scavenge is provided by including large drain passages throughout the test head. The intermediate bearing member (4) has a row of radial holes to permit centrifugally induced drainage of oil discharge from the inner side of the fluid-film bearing. Both the housing (6) and the sensor mounting ring (8) are provided with drain passages. Preliminary series hybrid bearing tests demonstrated that the free flow of lubricating oil into the shaft center was not being satisfactorily pumped into the bearings. A design review indicated the need for an internal shaft seal which is referred to as a modified feed tube. Figure 2 shows the new sealed feed tube assembly.

A floating ring seal (a), designed to have a small outer diameter clearance with the bore of the rotating shaft is positioned on the new stationary feed tube (b) by two end washers (c). A spacer ring (d) assures the proper seal ring clearance. The modified feed tube is firmly attached to the end cover (Item (7) of Figure 1) in a manner which permits the central feed lubricating oil supply to be continued. The introduction of the new central feed sealing system included the replacement of the shaft baffles (Item (12) of Figure 1) with a simple shaft plug (e). Two shear pins (f) were also included in the redesign of the test head as a safety feature to be used only during fluid-film bearing tests where rotation of the ball bearing is not desired. When activated, the shear pins engage slots machined into the

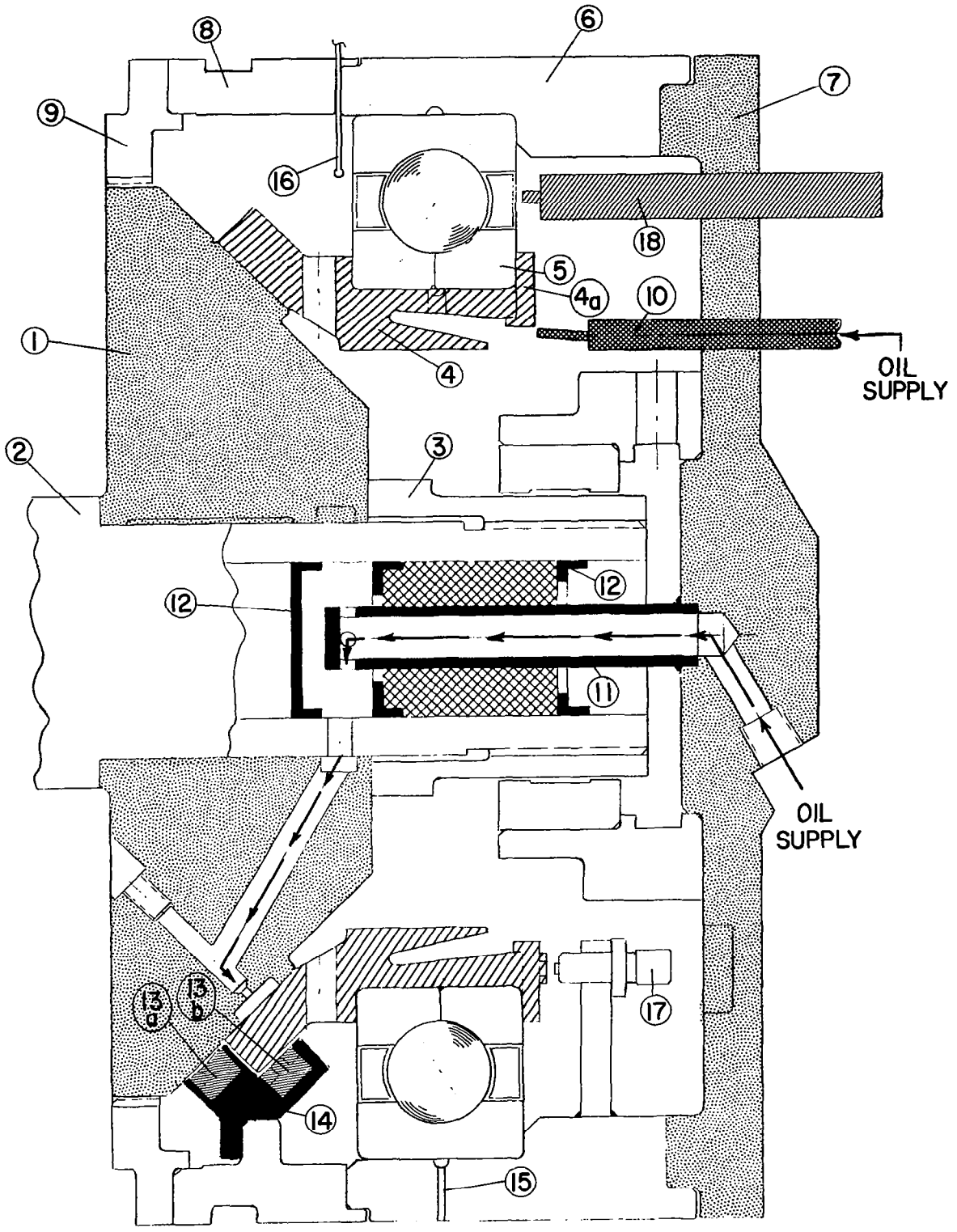

Fig. 1 Test Vehicle Head Assembly

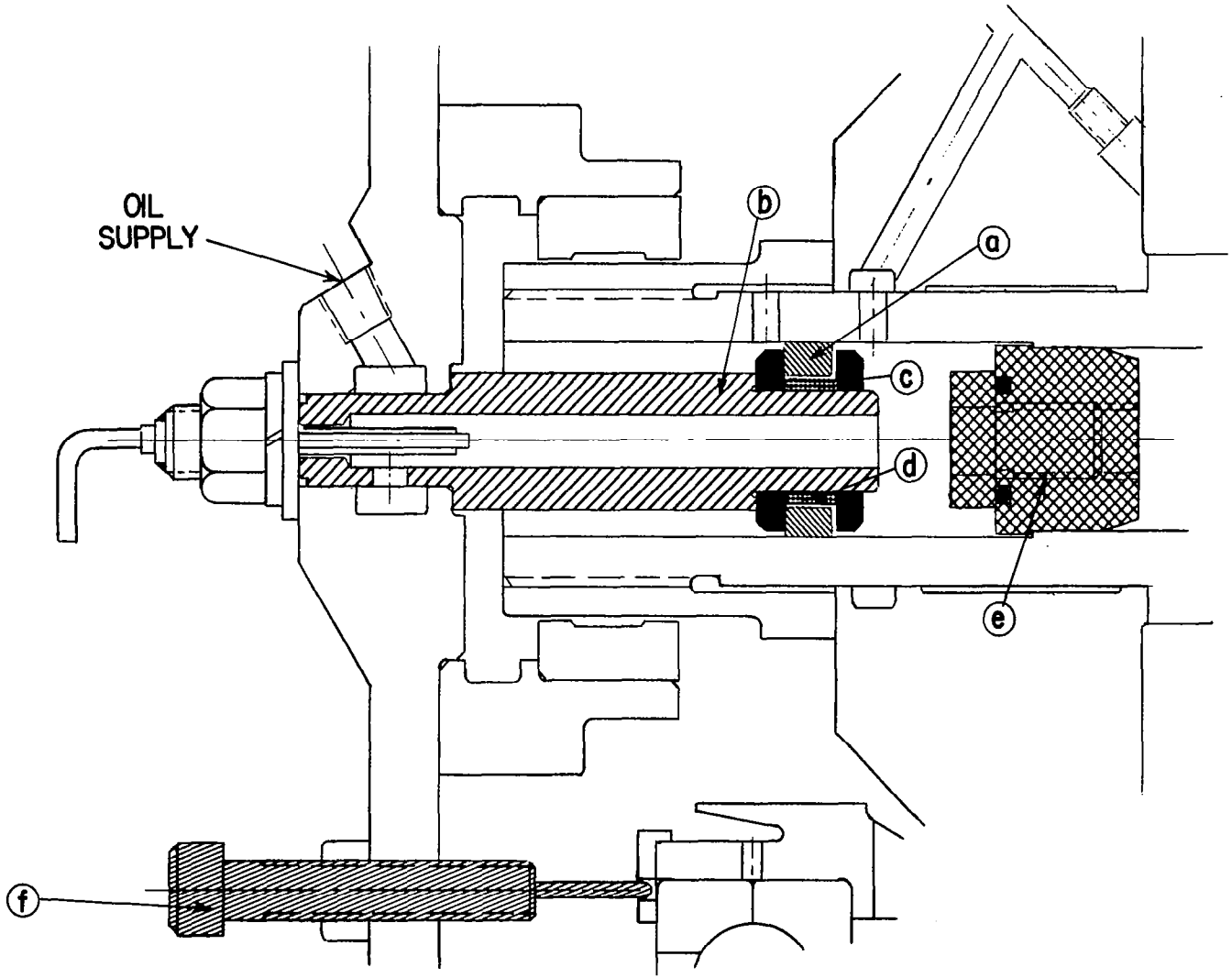

Fig. 2 Floating Ring Seal Installation

face of the bearing retainer (Item (4a) of Figure 1) and restrain the inner race and intermediate member (Item (4) of Figure 1) from rotating. In the event of an unintentional contact between the rotating and intermediate members, the shear pins would disengage thereby releasing the ball bearing. Free rotation of the ball bearing would prevent damage to the fluid-film bearing.

Photographs of machine parts are included in this report to provide a visual record of the more important test rig components. Figure 3, a close-up view of the conical fluid-film bearing runner, shows the pocket configuration and the position of the feed orifices. Figure 4 is a photograph of the intermediate bearing member. Identified on this photograph is the fluid-film bearing face, the inner diameter drain grooves, and a lubricant feed slot for the ball bearing. Figure 5, a partial view photograph of the assembled test head, shows the method of position sensor installation and the location of the original fluid-film bearing lubricant feed pipe. Figure 6 shows the redesigned feed pipe with the floating ring seal attached. Figures 7, 8 and 9 are included to show views of the installed conical bearing runner and spindle, the fully assembled and instrumented test head, and the fully installed test rig.

B. Test Instrumentation

A viable experimental program requires the use of sufficient instrumentation to fully determine the performance of the item undergoing test. For the series hybrid bearing tests, two categories of instrumentation are defined. One category is the dependent variable sensors. These instruments measure ball bearing outer race temperature, oil temperatures exiting both bearings, intermediate bearing member rotational speed, ball bearing cage speed, lubricant flow rate and ball bearing torque. The second instrumentation category consists of those instruments which measure the test vehicles independent variables including shaft rotational speed, test bearing lubricant supply temperature and pressure and the thrust load.

1. Dependent Variable Instrumentation

Instrumentation for measuring the dependent test variables are incorporated in the test head at the locations identified on Figure 1. Ball bearing and fluid-film bearing film thicknesses are measured by eddy current position sensors (13a) and (13b) mounted by pairs in probe holding blocks (14), which are securely fastened to the sensor mounting ring (8). Four probe pairs are employed for film thickness measurements and the four probe holders in which these probe pairs are epoxied, are positioned circumferentially every 90 degrees on lugs machined on the mounting ring. During test rig operation, changes in the relative position between the test ball bearing outer race and the fluid-film bearing runner are directly measured by probe (13a). The relative position between this ball bearing's outer race and the fluid-film bearing is provided by probe (13b). The difference between the readings of position sensors (13a) and (13b) at any test point relative to a known zero film thickness condition reading difference, provides the fluid-film bearing film thickness. To assure accurate film thickness

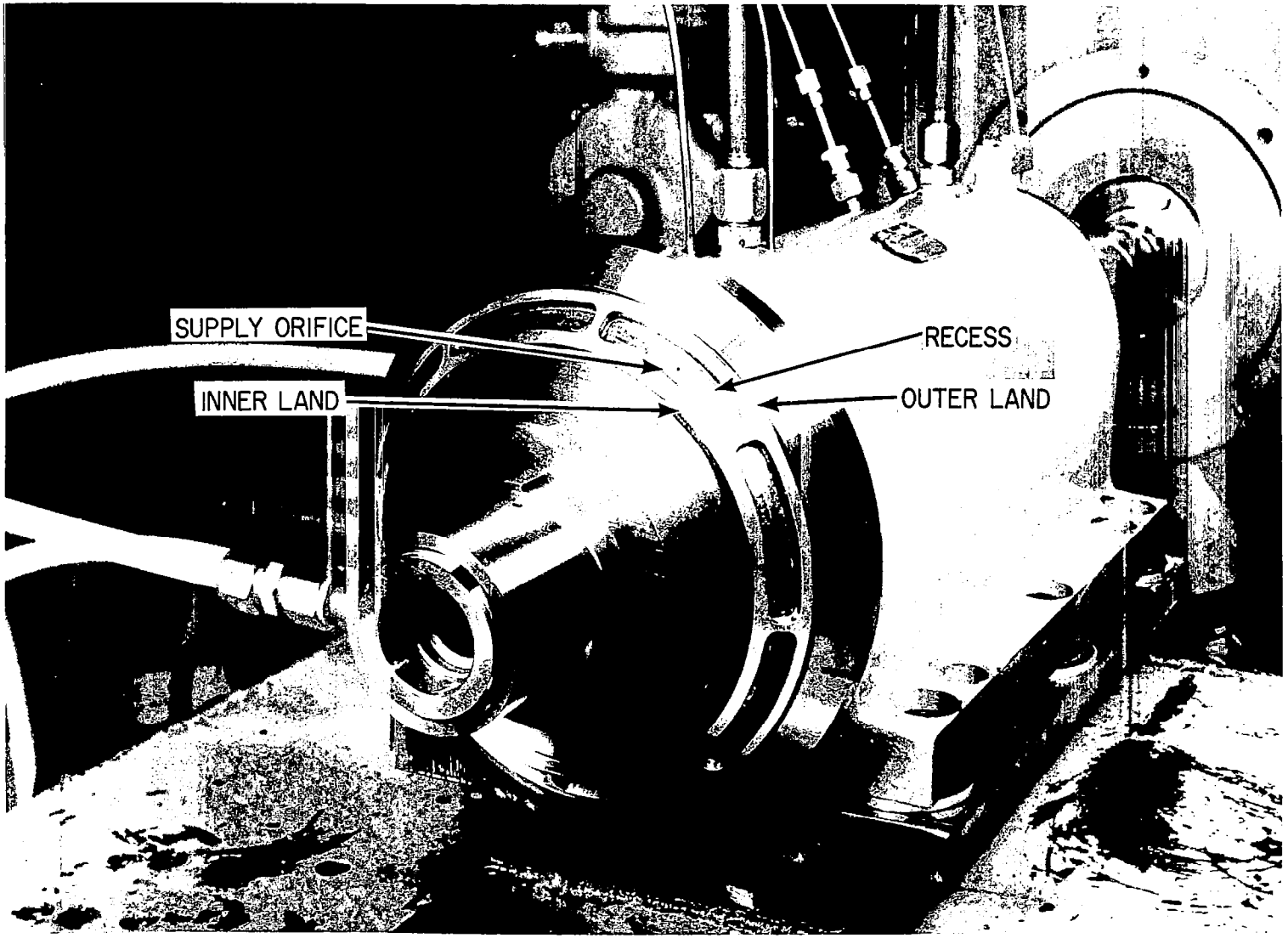

Fig. 3 Conical Fluid Film Bearing Runner

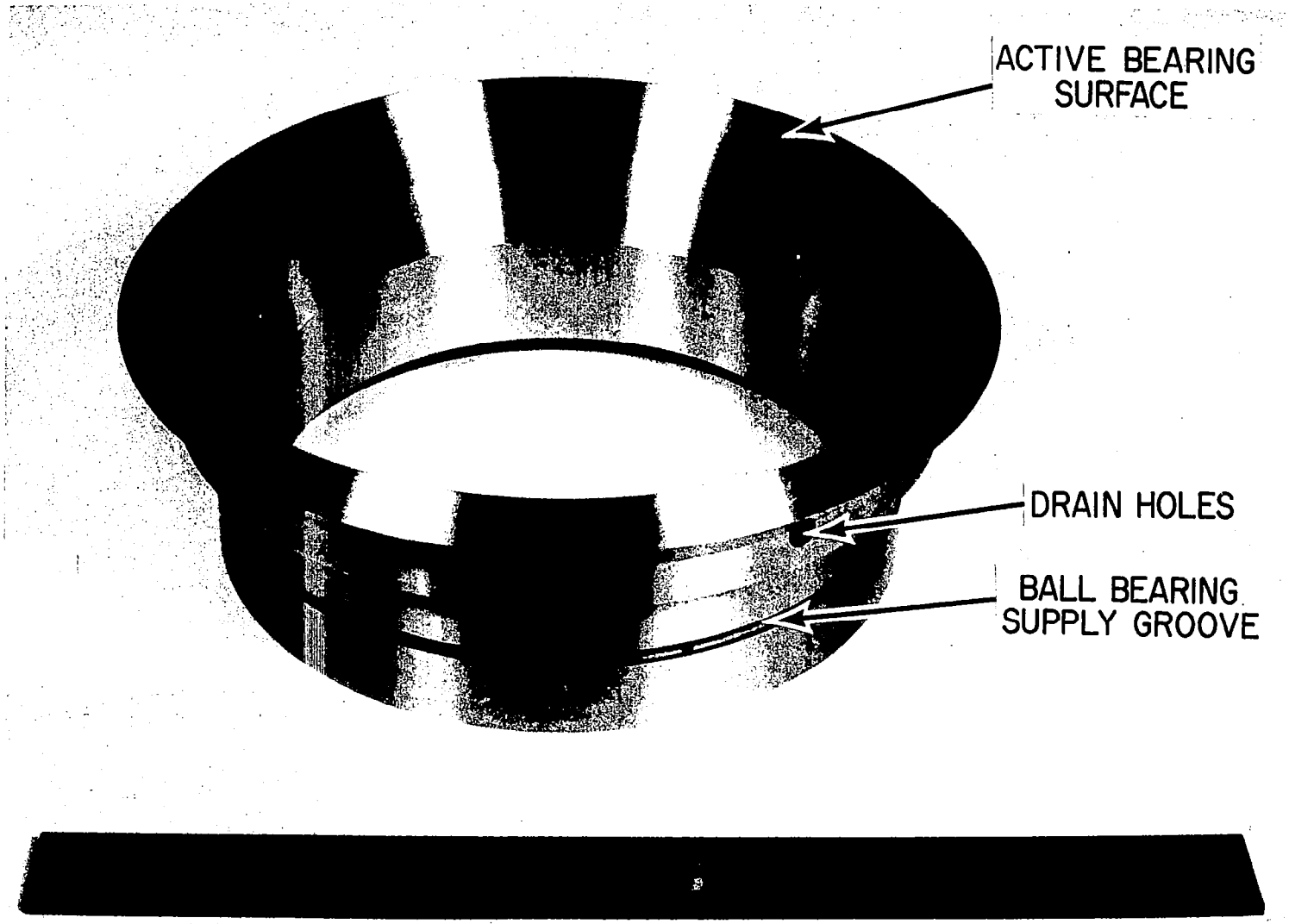

Fig. 4 Intermediate Bearing Member

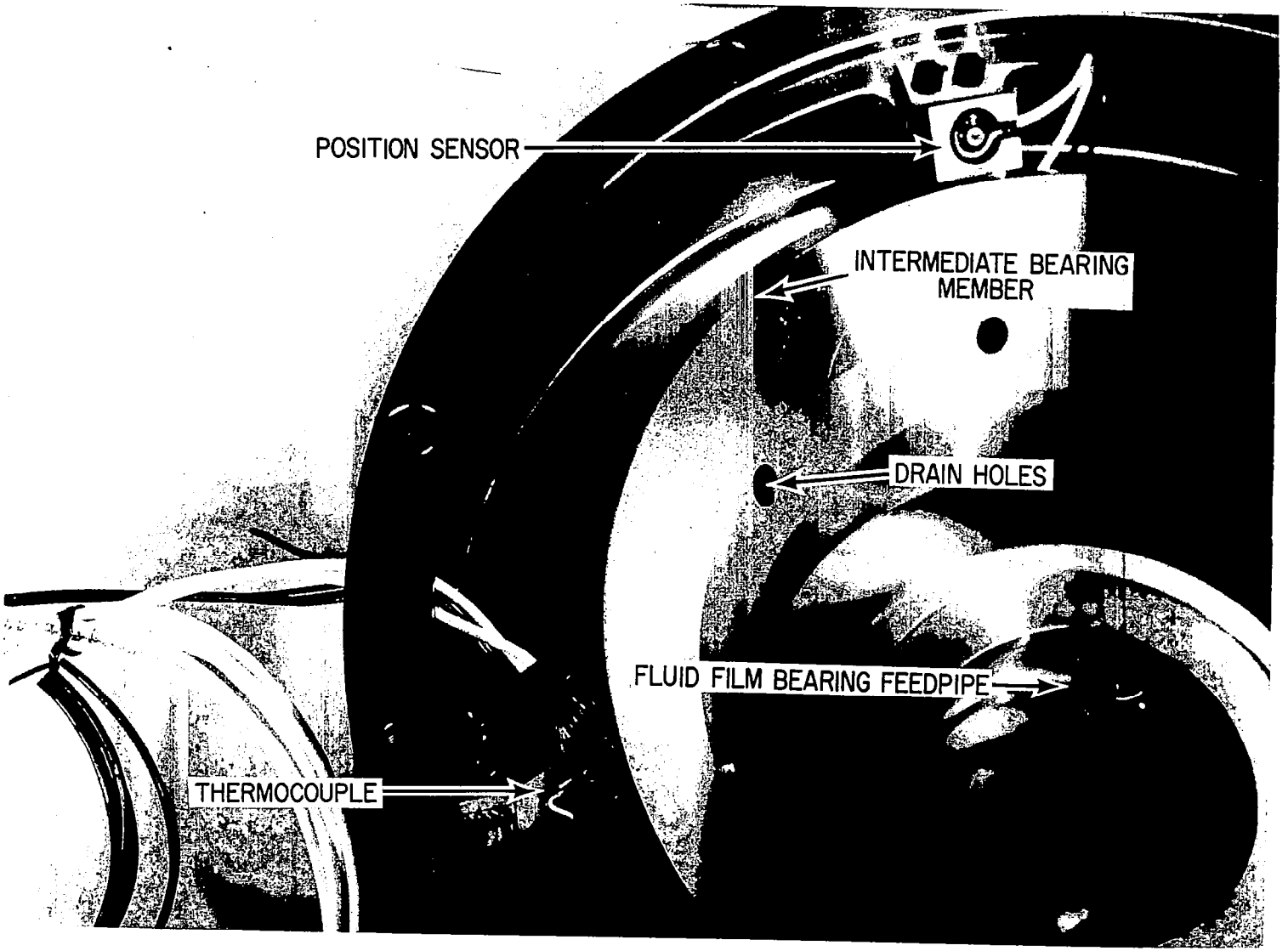

Fig. 5 Partial View of Assembled Test Head

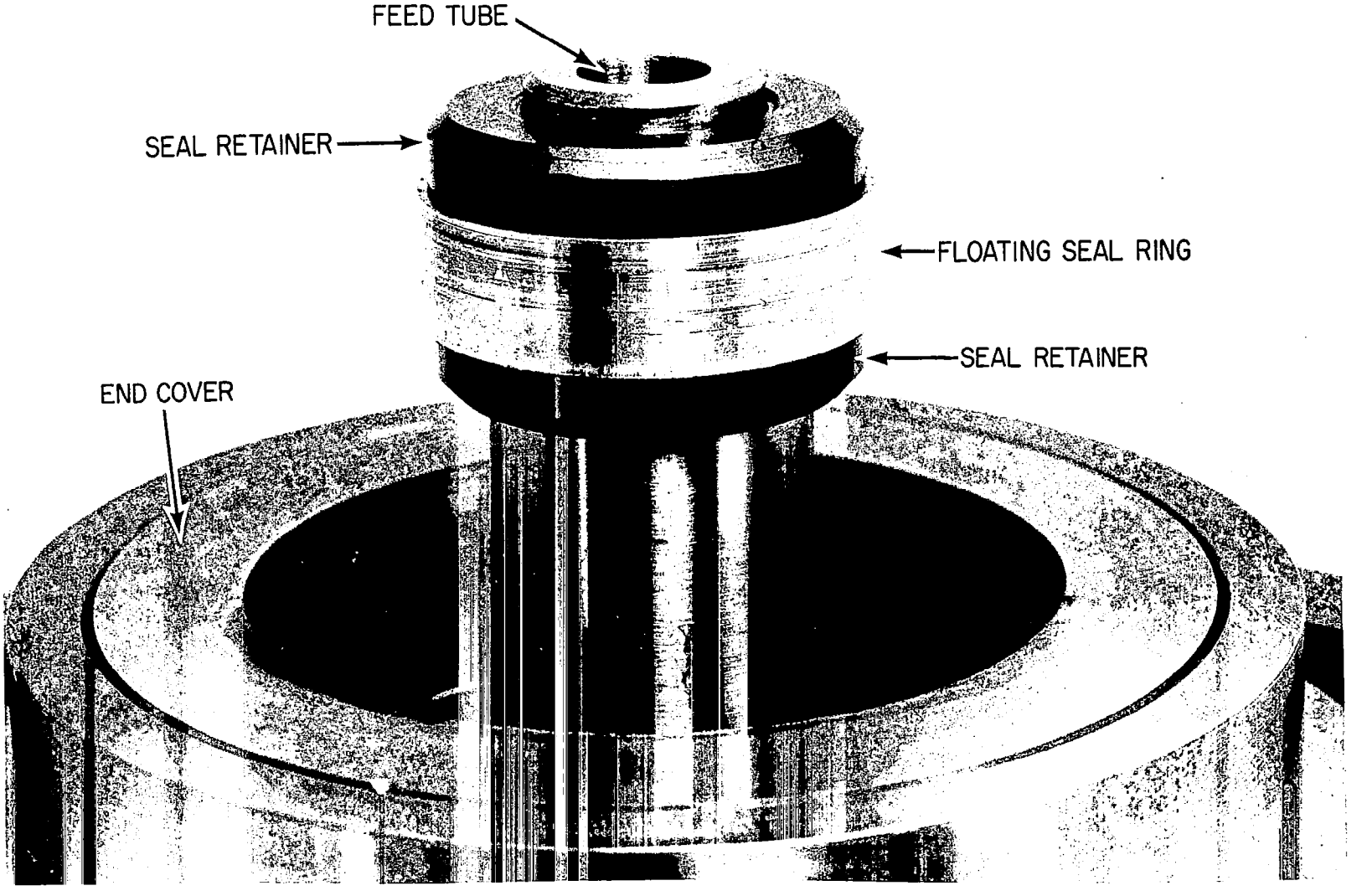

Fig. 6 Redesigned Oil Feed Pipe with Floating Ring Seal

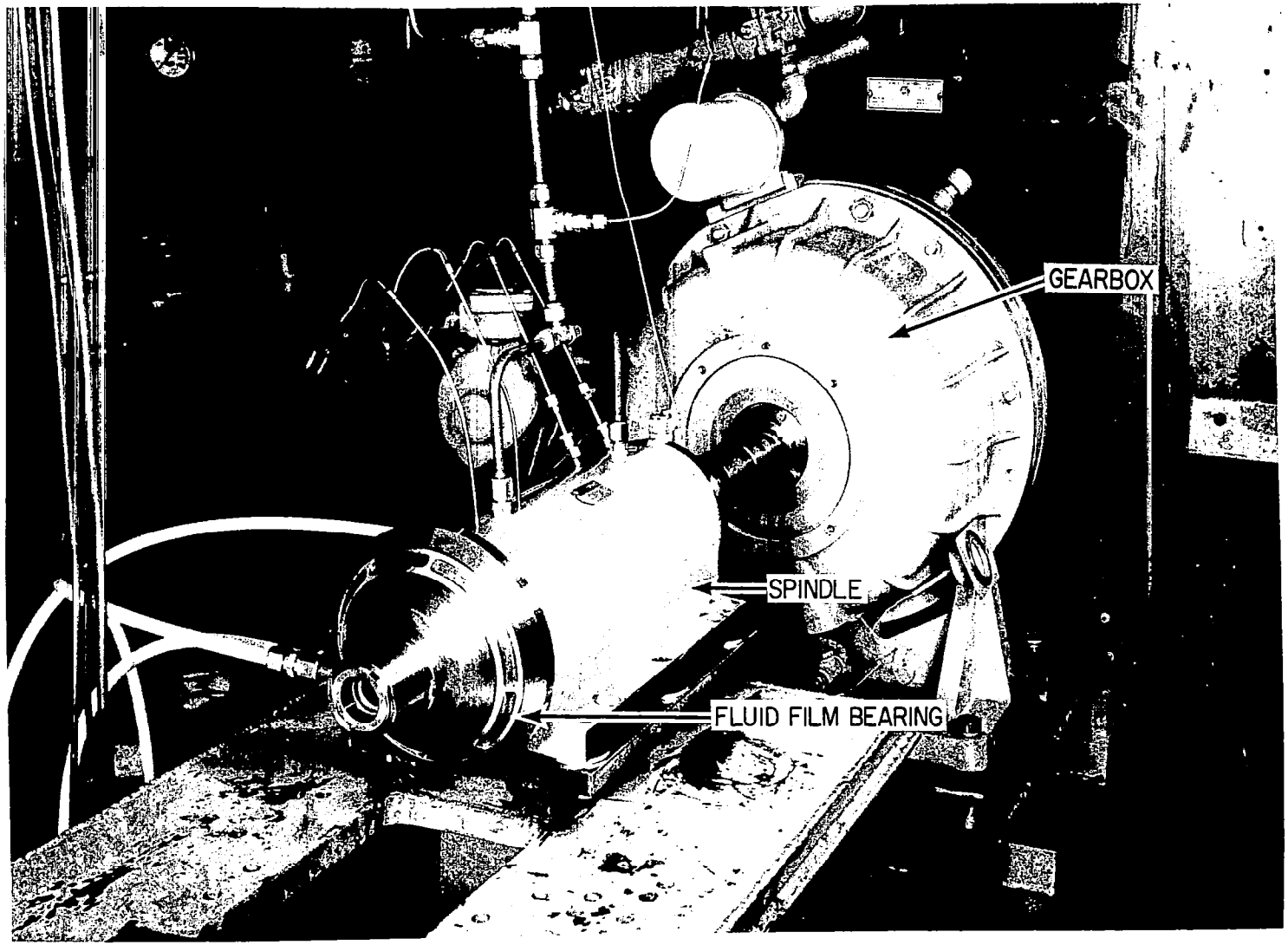

Fig. 7 Conical Bearing Runner and Spindle Installation

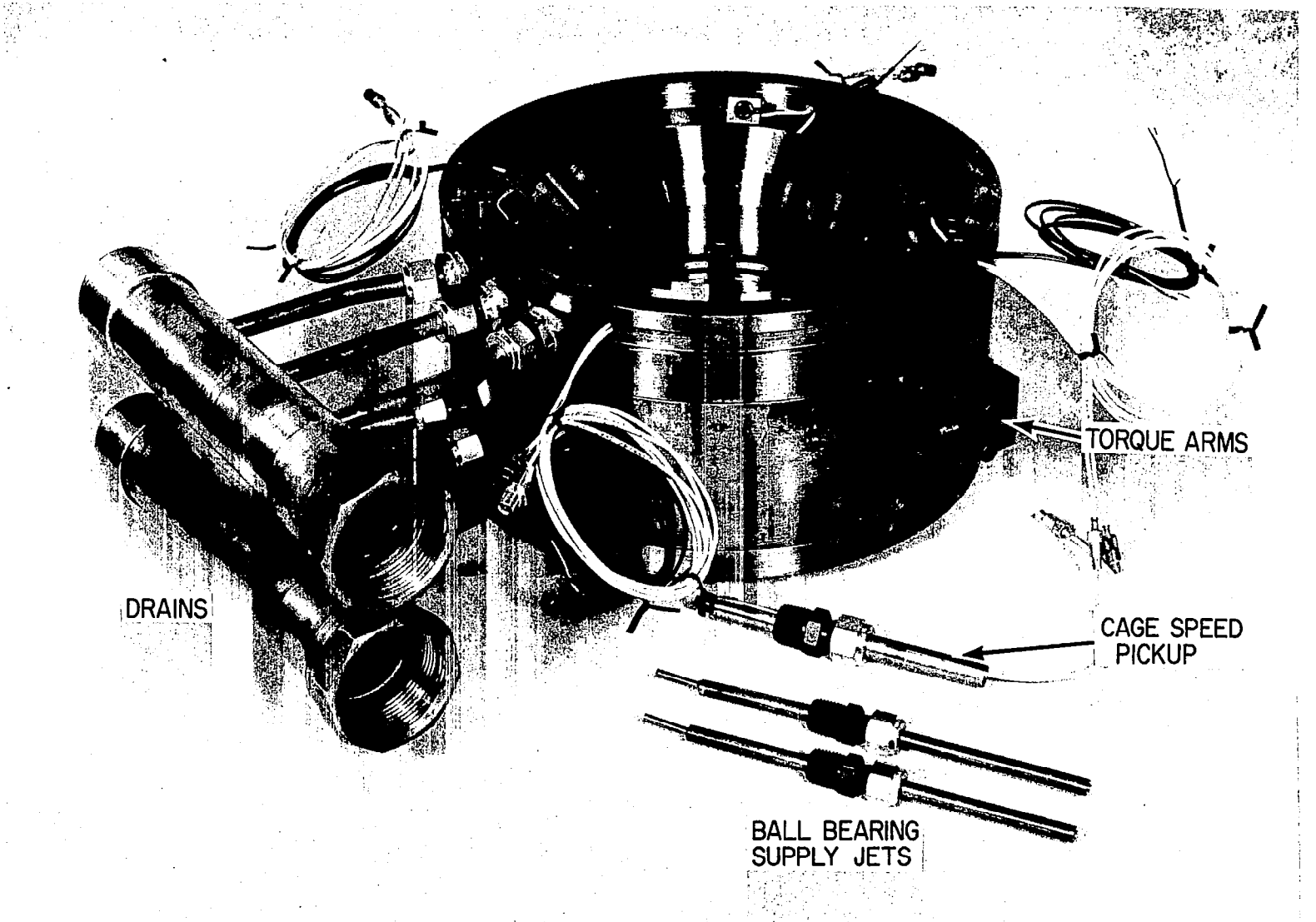

Fig. 8 Assembled Test Head

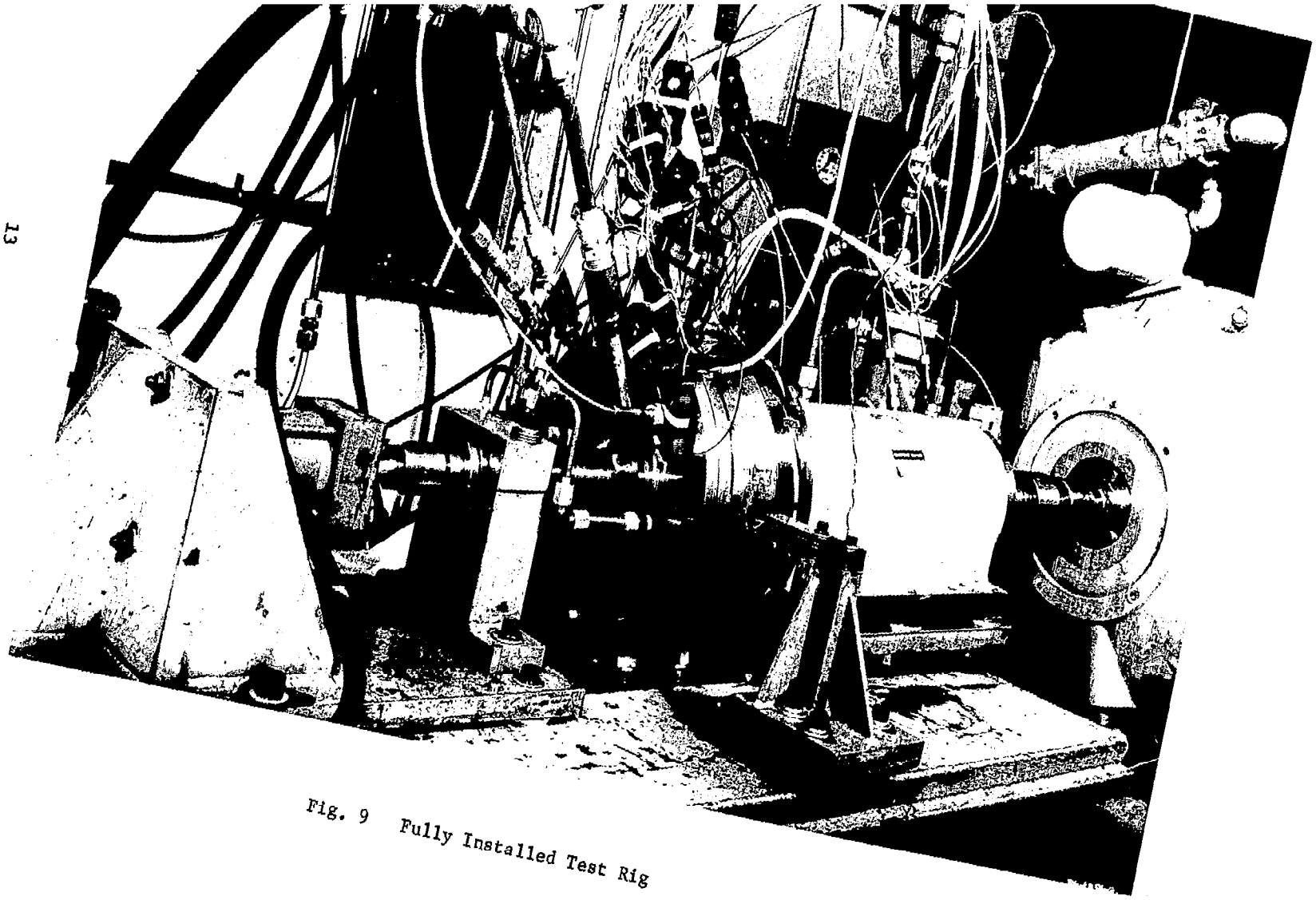

Fig. 9 Fully Installed Test Rig

measurements, each of the eight position sensors has an iron-constantan thermocouple installed with it. The thermocouple provides the temperature values required to compensate for true probe calibration. The location of the probe temperature thermocouples also makes them suitable for measurement of the oil discharge temperature at the fluid-film bearing.

Additional iron-constantan thermocouples are installed at various locations in the test head to ascertain other pertinent temperatures. Four thermocouples, identified as (15) in Figure 1, inserted at 90° intervals around the housing (6), are used to determine outer race ball bearing temperatures. A single thermocouple (16) is positioned to provide measurements of ball bearing lubricant discharge temperatures.

In addition to position and temperature measurement sensors, the test head is provided with two sensors for measuring speed. A magnetic pick-up (17) is used to determine the intermediate bearing member speed and an eddy current position sensing probe (18) is employed for ball bearing cage speed measurement. Additional test instrumentation locations are identified by Figure 10 and include instruments for the independent measurement of the lubricant flow rates and inlet temperatures to the ball bearing and fluid-film bearing. These instruments include two float type flow meters (3) and (4), two iron constantan thermocouples, (5) and (6), and a pressure gage (7). This gage is connected to a pressure tap which provides the measurement of the fluid-film bearing supply pressure.

The remaining dependent test variable is the level of torque produced by the rotation of either or both the fluid-film and ball bearing. This torque is measured by a pair of strain gage torque arms.

The torque arm arrangement is detailed in Reference [3]. Two torque arms are attached to the test rig housing. These arms contain balls which transmit the torque load by point contact onto deflection beams that are instrumented with strain gages. The beams are allowed to deflect a limited amount before they engage solid stops.

2. Independent Variable Instrumentation

Instruments to measure independent variables are also identified on Figure 10. These instruments are described as follows:

- A magnetic speed pick-up (1) which is positioned to view the spindle shaft at the end opposite the test bearing housing.
- Axial load is determined by the measurement of load cylinder pressure via a pressure gage (2).

C. Auxiliary Support Systems

Two major support systems were employed for the testing of the series hybrid bearing. These systems were the test vehicle drive and the lubricant

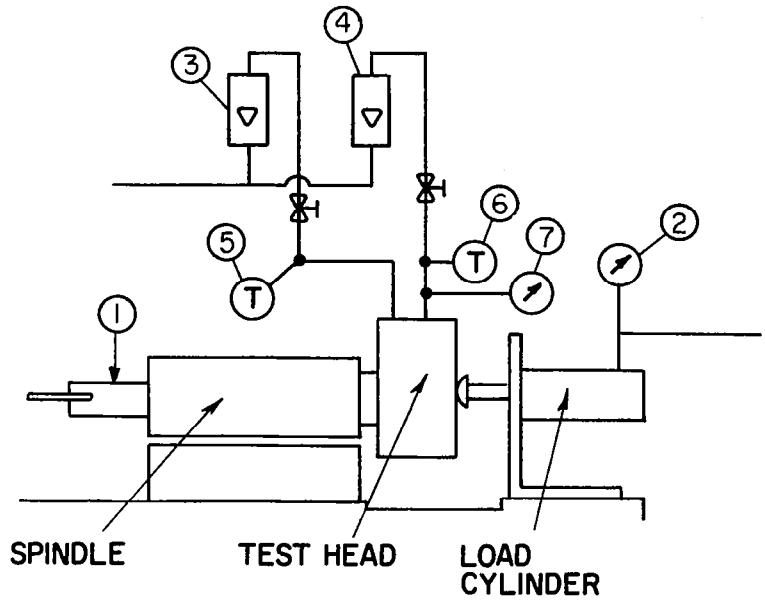

Fig. 10 Independent Variable Instrumentation

supply. Each system has been described previously in Reference [3] and, therefore, will only be briefly described here.

1. Drive System

Drive power is supplied to the test vehicle via a variable speed 7.46×10^4 Watt (100 HP) DC motor, coupled to a 6.34:1 step-up gear box. Gear box output shaft speeds over a continuously variable range of $1000 \leq \text{rpm} \leq 20{,}000$ are provided with this system.

2. Lubricant Supply System

Independent supply to both the fluid-film and ball bearing components of the series hybrid bearing are provided by a skid-mounted, lube oil system. This system can supply synthetic lubricants at pressures to 8.60×10^5 N/m^2 (125 lb/in^2), flow rates to 9.25×10^{-4}m^3/sec (13 gpm) and delivery temperatures up to 149°C (300°F). A second pumping unit, designed to supply only mineral oil, is capable of providing 6.31×10^{-3}m^3/sec (10 gpm) at 1.04×10^7 N/m^2 (1500 lb/in^2) and at delivery temperatures not to exceed 62.6°C (145°F).

III. EXPERIMENTAL RESULTS

The performance of the series hybrid bearing was evaluated on two separate set-ups, each one of which employed a different oil feeding method. The original set-up, shown in Figure 1, proved to be inadequate because of the excessive side leakage out of the shaft center. This set-up was subsequently revised as reflected in Figure 2. The revision consisted mainly of the introduction of a floating seal arrangement and a pressure tap into the shaft center. This modification has resulted in excellent flow control through the fluid-film bearing. In the following discussion, the results of both test set-up configurations will be analyzed. Also presented, is a description and analysis of the fluid-film bearing test series, which was designed to evaluate the performance of the fluid-film bearing at oil supply pressures, similar to those encountered in high-speed operation, but at much lower speed levels.

A. Test Results - Non-Sealed Lubricant Supply

In the initial test rig design, shown in Figure 1, oil to the fluid-film bearing was admitted through a stationary tube, located at the center of the rotating shaft. It was assumed that the oil injected between the baffles will be directly pumped out through the fluid-film bearing passages. To establish the flow rate required to sustain the fluid-film bearing in proper balance with the other conditions of operation, the flow had to be gradually increased until no further changes in film thickness occurred. When further increases in flow no longer increased film thicknesses that condition was assumed to be the point at which the flow requirements of the fluid-film bearing had been satisfied. This procedure was based on the assumption that the side leakage through the drilled baffle will be minimal. As will be shown later, this assumption proved to be erroneous and the maximum flow rate that could be pumped through the fluid-film bearing did not exceed $2.21 \times 10^{-4} m^3/sec$ (3.5 gpm) because of the side leakage effects.

The first test run on the set-up shown in Figure 1, was performed to establish the bearing system's characteristics at gradually increasing levels of load and speed. The conditions established prior to data acquisition were:

1. Ball Bearing Flow Rate
   Set at $6.31 \times 10^{-5} m^3/sec$ (1.0 gpm)

2. Fluid-Film Bearing Flow Rate
   Set at $2.21 \times 10^{-4} m^3/sec$ (3.5 gpm)

3. Lubricant
   Type 2 Ester (MIL-L-23699) and a Supply Temperature of 98°C (200°F)

4. Axial Load
   Set at 2224 N (500 lb)

At the above conditions, a minimum shaft rotational speed of 2,200 rpm was established and held until thermal equilibrium within the test head was reached. When thermal stability was obtained, rotor speed and axial load were increased sequentially until 10,000 rpm and a 4480 N (1000 lb) load was reached. At selected intervals during the above test, data was read and recorded. Reduction of this data is presented in Table I. This table lists the test identification number, the drive speed of the main shaft ω_s, the speed of the intermediate member ω_b, ω_b to ω_s ratio, the ball bearing cage speed, ω_c, the ratio of the cage speed to the intermediate member speed ω_c/ω_b, the axial load, the power input to the rotor drive, the power losses at the test head (includes fluid-film bearing loss, ball bearing loss and any associated churning losses in the bearing cavity), the temperature of the ball bearing outer races, and the fluid-film bearing film thickness, as measured by the built-in position sensors.

As is indicated by the data on Table I at the speed of 2,220 rpm, the fluid-film bearing still remained inoperative and the speed of the intermediate member was equal to that of the shaft. At about 3,500 rpm, the fluid-film bearing surfaces suddenly parted, establishing a separating oil film between the shaft and intermediate member. Simultaneously, with the parting of the fluid-film bearing surfaces, the ball bearing speed dropped to 42 percent of the shaft speed. This was observed on the intermediate speed indicator, as well as on the bearing cage speed indicator.

Subsequent attempts to raise the load carrying capacity by the introduction of more flow or through increases in speed resulted in effectively lower film thicknesses in the fluid-film bearing. This result was contrary to the normal expectations whereby an increase in speed should result in higher load carrying capabilities, i.e., provided that the flow requirements are satisfied. The increase in flow did produce, however, higher churning losses, as measured on the test head. This indicated that the flow supplied to the test head did not fully find its way up to the film bearing. In order to verify this hypothesis, the test rig was disassembled and the intermediate, as well as the ball bearing members removed from the set-up. The end cover plate was replaced with a transparent lucite plate which contained at the center the oil feed tube.

The verification test consisted of the introduction of oil into the center of the shaft and observation of the intensity of the oil jets emanating from the hydrostatic bearing orifices, as well as the oil rejection pattern emanating from the front end of the rotating shaft. The speed of the test rig was brought up to 10,000 rpm and oil introduced at flow rates varying from 0 to $3.78 \times 10^{-4} m^3/sec$ (0 to 6 gpm). It was noted that with the shaft rotating at 10,000 rpm, the gradual increase in oil flow through the shaft center tube from 0 to $1.89 \times 10^{-4} m^3/sec$ (0 to 3 gpm) produced no end leakage of the shaft and resulted in gradual increase in intensity of the oil flow through the orifices. When, however, the oil flow was increased beyond 3.5 gpm, the shaft end leakage became apparent. Any further increases in the oil resulted in an apparent increase of shaft end leakage with the oil discharging from the fluid-film bearing orifices remaining approximately at the same intensity. These observations were made with the use of a

TABLE I

TEST SEQUENCE 1.0 - 10,000 RPM
SERIES HYBRID BEARING

Test Ident. No.	Drive Speed ω_s rpm	Inter-mediate Member Speed ω_b rpm	ω_b/ω_s	Cage Speed ω_c rpm	ω_c/ω_b	Axial Load N (lb)	Input Power Watts (HP)	Test Head Losses Watts (HP)	Ball Brgs. Outer Races Temp °C(°F)	Fluid-Film Brg. Film Thickness 10^{-2}mm(10^{-3}in)
1-1	2220	2220	1	1021	.46	2224 (500)	1000 (1.34)		95.6 (204)	
1-2	4560	1915	.42	862	.45	2224 (500)	3000 (4.03)	805 (1.08)	97.2 (207)	3.89 (1.53)
1-3	7380	3100	.42	1430	.46	2980 (671)	5000 (6.70)	2490 (3.34)	99.4 (211)	3.56 (1.40)
1-4	9120	3830	.42	1760	.46	3890 (875)	7000 (9.40)	4530 (6.06)	102.8 (217)	3.10 (1.22)
1-5	10000	4435	.44	2040	.46	4448(1000)	8500 (11.4)	6160 (8.26)	105 (221)	3.74 (1.08)

Lubricant Flow Rate: BB = 6.31×10^{-5} m^3/sec (1.0 gpm)

FF = 2.21×10^{-4} m^3/sec (3.5 gpm)

Lubricant Supply Temp: BB = 92.8°C(199°F)

FF = 95.6°C(204°F)

strobe light which maintained the rotor at a "stand-still" for purposes of observations while the shaft was rotating at 10,000 rpm. At this point, the indications were clear that unless some positive sealing arrangement was obtained for the oil feed tube, the excessive side leakage exiting from the shaft end will not permit the achievement of higher speeds or higher loads during the test sequence.

Prior to final disassembly, system oil failure was simulated (fail-safe test) at a speed of 10,000 rpm and a 4448 N (1000 lb) axial load, by stopping the oil flow to the fluid-film bearing several times. Each time the oil flow to the fluid bearing was terminated, the ball bearing inner race accelerated quickly to the shaft speed level without any audible changes in the system performance. Similarly, the restoration of oil flow to the fluid-film bearing with the shaft speed maintained at 10,000 rpm resulted in fluid-film bearing activation and a reduction of the ball bearing speed to 43 percent of the shaft speed - an excellent speed split. In the oil system failure tests, the ball bearing temperature would stabilize at 105°C (220°F) when the fluid-film bearing was activated. At the time of oil shutdown to the fluid-film bearing, the temperature of the outer race of the ball bearing rose to 128°C (265°F). This increase in outer race temperature was mainly due to the increase in the effective ball bearing speed.

Tear-down and inspection of the bearing after the fail-safe series of tests showed the fluid-film bearing and the ball bearing to be in excellent condition. Figures 11 and 12 show close-up photographs of the conical bearing runner and the active face of the intermediate bearing member. The bearing surfaces of the runner and the intermediate member show some circumferential scratches and burnishes, but not of sufficient magnitude to affect their performance.

B. Test Results Using the Sealed Shaft Oil Systems

It was evident from the results of the early hybrid bearing tests that the original oil feeding system could not assure sufficient lubricant flow to sustain the fluid-film bearing requirements. The installation of the sealed oil supply in combination with provisions for measuring the pressure of the oil entrained within the shaft provided two important benefits; namely, the ability to supply larger volumes of the lubricants to the fluid-film bearing (if necessary, by pressurizing), as well as the ability to read the pressure in the shaft at the point where the oil is introduced into the radial passages leading to the bearing pads.

The supply of the larger volumes of pressurized oil now afforded the opportunity of checking the fluid-film bearing behavior at lower speeds but at pressures simulating those centrifugally developed at higher speeds. Furthermore, the direct readings of the pressure inside the shaft provided a positive identification of a continual presence of oil in this area. In other words, as long as the flow to the fluid-film bearing was satisfied, the inner shaft volume remained at a positive pressure. As soon as that pressure was at or reached below zero, one could safely surmise that the flow requirements to the fluid-film bearing are not going to be satisfied.

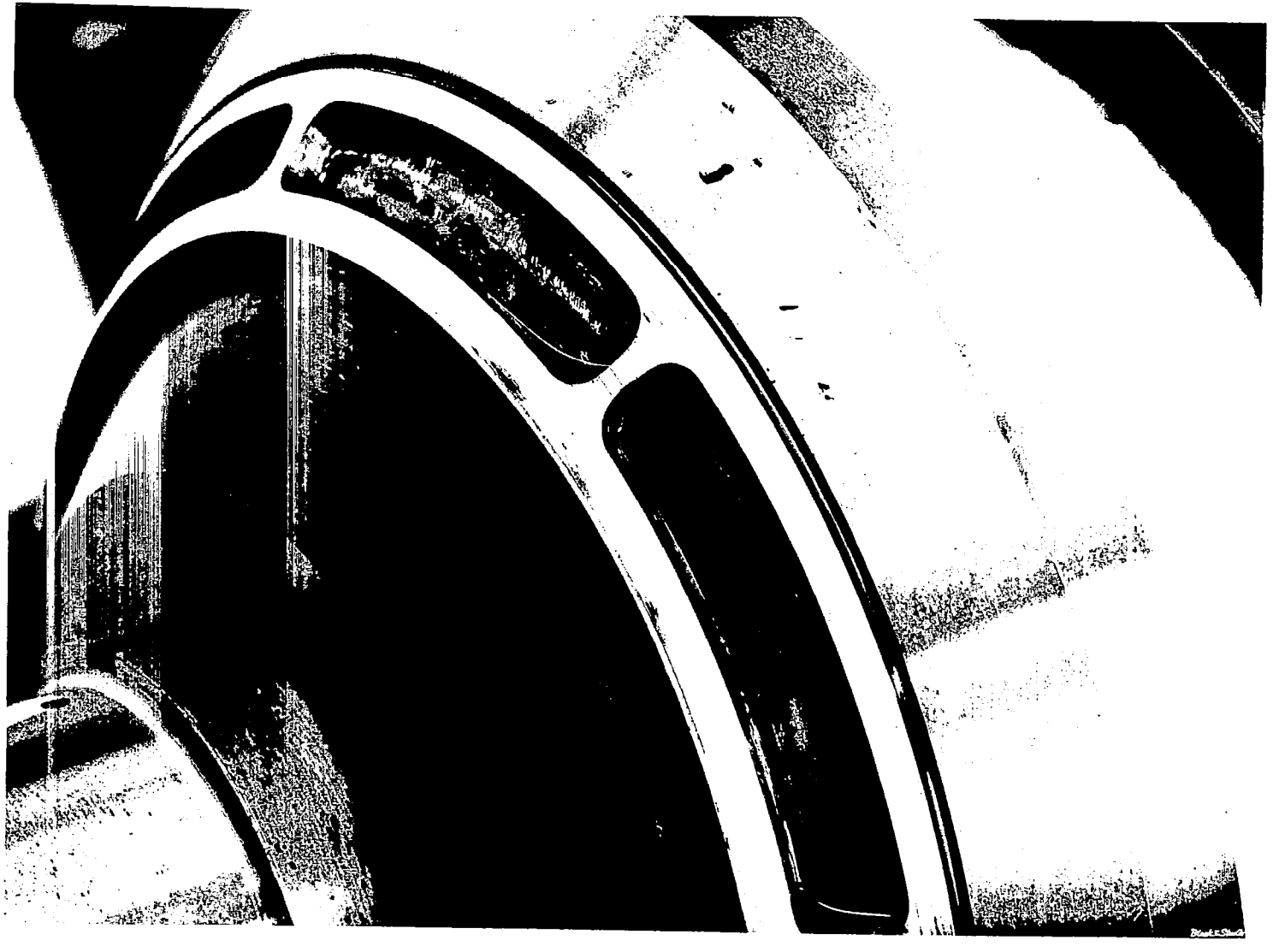

Fig. 11 Conical Fluid Film Bearing Runner - Fail-Safe Test

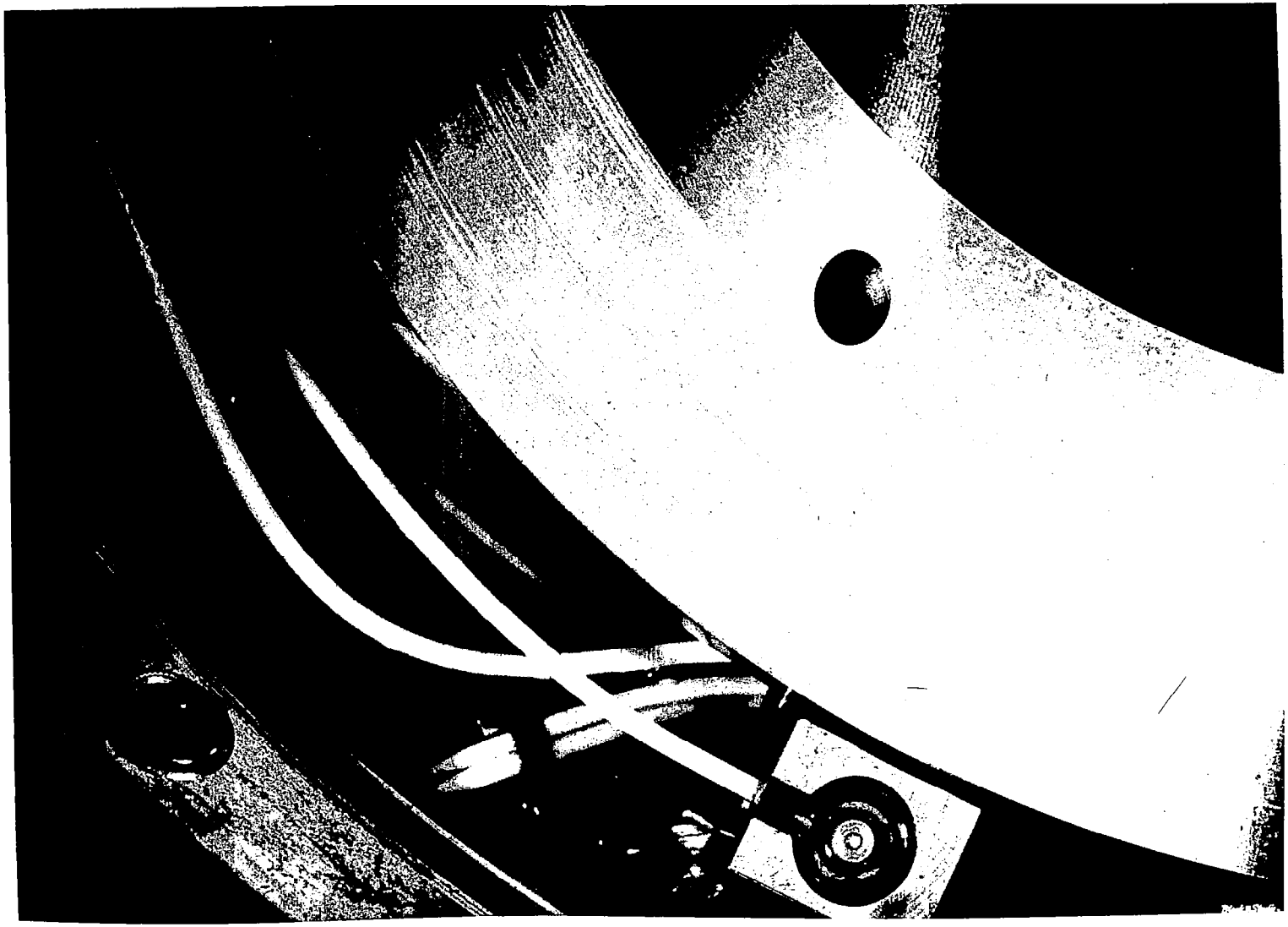

Fig. 12 Intermediate Bearing Member Fail-Safe Test

Table II lists the targeted test plan made possible with the use of a sealed oil supply. The new test sequence 1.0 establishes the ball bearing deflection characteristics required when extracting fluid-film bearing thicknesses from the test data.

Test sequences 2.0 through 4.0 establish the performance of the fluid-film bearing component. The remaining test sequence, 5.0, provides data related to the performance of the full series hybrid bearing set-up.

The initial work plan called for the fluid-film bearing evaluation to be performed using a Type 2 ester (MIL-L-23699) lubricant. Preliminary runs with the high pressure lubricant supply system disclosed that the available system was not capable of operating on the synthetic ester type oil at temperatures of 200°F. As a result of this restriction, the tests of the fluid-film bearing only were performed using a SAE-10 mineral oil. The hybrid bearing tests were conducted using the specified MIL-L-23699 lubricant.

1. Fluid-Film Bearing Tests

The fluid-film bearing test series was performed to establish the load carrying capacity of the fluid-film bearing component when subjected to hydrostatic action resulting from an externally pressurized source. Since the actual pressures generated during hybrid bearing operation could not be measured (because of the rotation of both fluid-film bearing faces), a comparison between the load carrying capacity of the externally pressurized bearing with that of a centrifugally fed bearing could provide valuable information regarding the efficiency of the centrifugal-feed approach.

The fluid-film bearing evaluation consisted of tests at rotor speeds of 0, 2000 rpm, 4000 rpm, 6000 rpm and 8000 rpm, with hydrostatic supply pressures of 251 x 10^4 N/m^2 (364 lb/in^2), 569 x 10^4 N/m^2 (825 lb/in^2), and 1010 x 10^4 N/m^2 (1,465 lb/in^2) corresponding to hydraulic pressures developed at 10,000 rpm, 15,000 rpm and 20,000 rpm of shaft rotation. The applied load varied between 2224 N (500 lb) to 17792 N (4000 lb), depending upon the load carrying capability of the bearings.

The results of the tests are summarized in Table III. Of primary interest in these tests, are the effect of speed, load, and hydrostatic supply pressure on the film thickness, torque, and oil flow rates.

Graphical representations of the fluid-film bearing test results are presented in Figures 13 through 15. Figure 13 shows the results for data point 2.0 (hydrostatic pressure corresponding to a 10,000 rpm shaft speed). Figure 14 depicts the test results for data point 3.0 (hydrostatic pressure corresponding to a shaft speed of 15,000 rpm), and Figure 15, results of runs with hydrostatic pressures corresponding to a shaft speed of 20,000 rpm (data point 4.0).

The comparison between the experimentally and analytically produced data indicates several important results. First, on an average basis, the experimentally measured change in the film thickness with load (or

TABLE II

AMENDED TEST SEQUENCE - FLUID-FILM & SERIES HYBRID BEARING EVALUATION

1.0 No Lubricant Supply To Fluid-Film Bearing

1.1	External Load Set To	2,224 N (500 lb)
1.2	" " " "	4,448 N (1000 lb)
1.3	" " " "	8,896 N (2000 lb)
1.4	" " " "	13,344 N (3000 lb)
1.5	" " " "	17,792 N (4000 lb)

2.0 Lubricant Supply Pressure Set Equivalent to Centrifugal Pumping Speed of 10,000 RPM; 2.51×10^6 N/m^2 (364 lb/in^2)

2.1 External Load Set to 2,224 N (500 lb)

2.1.1 Thru 2.1.4 Shaft Speed of 2000,4000, 6000 & 8000 rpm

2.2 External Load Set to 4,448 N (1000 lb)

2.2.1 Thru 2.2.4 Shaft Speed of 2000,4000, 6000 & 8000 rpm

2.3 External Load Set to 6,672 N (1500 lb)

2.3.1 Thru 2.3.4 Shaft Speed of 2000,4000, 6000 & 8000 rpm

3.0 Lubricant Supply Pressure Set Equivalent to Centrifugal Pumping Speed of 15,000 RPM; 5.69×10^6 N/m^2 (825 lb/in^2)

3.1 External Load Set to 4,448 N (1000 lb)

3.1.1 Thru 3.1.4 Shaft Speed of 2000,4000, 6000 & 8000 rpm

3.2 External Load Set to 6,672 N (1500 lb)

3.2.1 Thru 3.2.4 Shaft Speed of 2000,4000, 6000 & 8000 rpm

3.3 External Load Set to 8,896 N (2000 lb)

3.3.1 Thru 3.3.4 Shaft Speed of 2000,4000, 6000 & 8000 rpm

3.4 External Load Set to 11,120 N (2500 lb)

3.4.1 Thru 3.4.4 Shaft Speed of 2000,4000, 6000 & 8000 rpm

TABLE II(Cont'd.)

4.0 Lubricant Supply Pressure Set Equivalent to Centrifugal Pumping Speed of 20,000 RPM; 1.01×10^7 N/m^2 (1465 lb/in^2)

4.1 External Load Set to 4,448 N (1000 lb)

4.1.1 Thru 4.1.4 Shaft Speed of 2000, 4000, 6000 & 8000 rpm

4.2 External Load Set to 8,896 N (2000 lb)

4.2.1 Thru 4.2.4 Shaft Speed of 2000, 4000, 6000 & 8000 rpm

4.3 External Load Set to 13,344 N (3000 lb)

4.3.1 Thru 4.3.4 Shaft Speed of 2000, 4000, 6000 & 8000 rpm

4.4 External Load Set to 17,792 N (4000 lb)

4.4.1 Thru 4.4.4 Shaft Speed of 2000, 4000, 6000 & 8000 rpm

5.0 Series Hybrid Bearing System Tests

5.1 Shaft Speed Set at 10,000 rpm
External Load Set at 4,448 N (1000 lb)

5.2 Shaft Speed Set at 15,000 rpm
External Load Set at 4,448 N (1000 lb) and 8,896 N (2000 lb)

5.3 Shaft Speed Set at 20,000 rpm
External Load Set at 4,448 N (1000 lb), 8,896 N (2000 lb), 13,344 N (3000 lb), and 17,792 N (4000 lb)

TABLE III

FLUID-FILM BEARING COMPONENT EXPERIMENTAL RESULTS

Data Point	External Load N (lb)	Rotor Speed rpm	Lubricant Supply Pressure 10^4 N/m^2 (lb/in^2)	Lubricant Supply Temp. °C (°F)	Lubricant Flow Rate 10^{-6} m^3/sec (gpm)	Film* Thickness 10^{-5} m (10^{-3} in)	Bearing Torque N-m (in-lb)	Bearing Power Watts (HP)	Lubricant Discharge Temperature °C (°F)
1.1.0	2224 (500)	0	- -	- -	- -	-.41 (-.16)	- -	- -	60.0 (140)
1.2.0**	4448 (1000)	0	- -	- -	- -	0 (0)	- -	- -	59.5 (139)
1.3.0	8896 (2000)	0	- -	- -	- -	1.30 (0.52)	- -	- -	58.8 (138)
1.4.0	13344 (3000)	0	- -	- -	- -	2.21 (0.87)	- -	- -	59.5 (139)
1.5.0	17792 (4000)	0	- -	- -	- -	3.48 (1.37)	- -	- -	59.5 (139)
2.1.0	2224 (500)	0	251 (364)	59.4 (139)	2.71 (4.3)	7.75 (3.05)	- -	- -	60.0 (140)
2.1.1	2224 (500)	2000	251 (364)	59.4 (139)	2.78 (4.4)	6.81 (2.68)	- -	- -	62.2 (144)
2.1.2	2224 (500)	4000	251 (364)	60.0 (140)	2.90 (4.6)	6.50 (2.56)	- -	- -	64.4 (148)
2.1.3	2224 (500)	6000	251 (364)	60.5 (141)	3.15 (5.0)	6.35 (2.50)	1.81 (16.0)	2135 (1.52)	68.9 (156)
2.1.4	2224 (500)	8000	251 (364)	63.3 (146)	3.41 (5.4)	6.27 (2.47)	4.06 (36.0)	3400 (4.56)	74.4 (166)
2.2.0	4448 (1000)	0	251 (364)	65.0 (149)	2.59 (4.1)	4.44 (1.75)	- -	- -	67.8 (154)
2.2.1	4448 (1000)	2000	251 (364)	63.3 (146)	2.65 (4.2)	4.44 (1.75)	- -	- -	66.7 (152)
2.2.2	4448 (1000)	4000	251 (364)	61.7 (143)	2.90 (4.6)	5.08 (2.00)	- -	- -	66.7 (152)
2.2.3	4448 (1000)	6000	251 (364)	61.1 (142)	3.09 (4.9)	4.37 (1.72)	2.26 (20.0)	746 (1.0)	71.1 (160)
2.2.4	4448 (1000)	8000	251 (364)	61.1 (142)	3.41 (5.4)	4.44 (1.75)	4.52 (40.0)	3810 (5.1)	75.6 (168)
2.3.0	6672 (1500)	0	251 (364)	64.4 (148)	2.08 (3.3)	3.43 (1.35)	- -	- -	66.7 (152)
2.3.1	6672 (1500)	2000	251 (364)	63.3 (146)	2.21 (3.5)	3.56 (1.40)	- -	- -	66.7 (152)
2.3.2	6672 (1500)	4000	251 (364)	62.2 (144)	2.46 (3.9)	3.81 (1.50)	- -	- -	67.8 (154)
2.3.3	6672 (1500)	6000	251 (364)	61.1 (142)	2.90 (4.6)	3.68 (1.45)	2.44 (21.6)	1570 (2.1)	71.1 (160)
2.3.4	6672 (1500)	8000	251 (364)	61.7 (143)	3.28 (5.2)	3.86 (1.52)	5.17 (45.8)	4340 (5.81)	76.7 (170)
3.1.0	4448 (1000)	0	569 (825)	58.9 (138)	4.10 (6.50)	6.17 (2.43)	- -	- -	59.4 (139)
3.1.1	4448 (1000)	2000	569 (825)	61.1 (142)	4.20 (6.65)	5.66 (2.23)	- -	- -	60.0 (140)
3.1.2	4448 (1000)	4000	569 (825)	60.0 (140)	4.26 (6.75)	5.44 (2.14)	- -	- -	62.2 (144)
3.1.3	4448 (1000)	6000	569 (825)	61.1 (142)	4.38 (6.95)	5.08 (2.00)	1.21 (10.7)	754 (1.01)	66.7 (152)
3.1.4	4448 (1000)	8000	569 (825)	61.7 (143)	4.60 (7.30)	4.83 (1.90)	4.56 (40.4)	3820 (5.12)	72.2 (162)
3.2.0	6672 (1500)	0	569 (825)	62.2 (144)	4.19 (6.65)	4.44 (1.75)	- -	- -	64.4 (148)
3.2.1	6672 (1500)	2000	569 (825)	58.9 (138)	4.19 (6.65)	4.83 (1.90)	- -	- -	63.9 (147)
3.2.2	6672 (1500)	4000	569 (825)	58.9 (138)	4.22 (6.70)	4.14 (1.63)	- -	- -	64.4 (148)
3.2.3	6672 (1500)	6000	569 (825)	60.0 (140)	4.38 (6.95)	5.05 (1.99)	2.58 (22.9)	1630 (2.18)	67.7 (154)
3.2.4	6672 (1500)	8000	569 (825)	58.9 (138)	4.67 (7.40)	4.85 (1.91)	5.32 (47.2)	4460 (5.99)	72.2 (162)
3.3.0	8896 (2000)	0	569 (825)	61.1 (142)	4.10 (6.50)	3.91 (1.54)	- -	- -	65.6 (150)
3.3.1	8896 (2000)	2000	569 (825)	60.0 (140)	4.09 (6.48)	3.63 (1.43)	- -	- -	63.3 (146)
3.3.2	8896 (2000)	4000	569 (825)	58.9 (138)	4.10 (6.50)	3.56 (1.40)	0.30 (2.70)	127 (0.17)	65.6 (150)
3.3.3	8896 (2000)	6000	569 (825)	58.9 (138)	4.32 (6.85)	3.66 (1.44)	3.35 (28.3)	2010 (2.69)	68.9 (156)
3.3.4	8896 (2000)	8000	569 (825)	59.4 (139)	4.57 (7.25)	3.61 (1.42)	6.08 (51.2)	4850 (6.50)	73.3 (164)
3.4.0	11120 (2500)	0	569 (825)	62.2 (144)	3.91 (6.20)	3.73 (1.47)	- -	- -	66.7 (152)
3.4.1	11120 (2500)	2000	569 (825)	61.1 (142)	3.91 (6.20)	3.40 (1.34)	- -	- -	65.6 (150)
3.4.2	11120 (2500)	4000	569 (825)	60.5 (141)	3.91 (6.20)	3.45 (1.36)	0.30 (2.70)	127 (0.17)	67.2 (153)
3.4.3	11120 (2500)	6000	569 (825)	60.0 (140)	4.23 (6.70)	3.38 (1.33)	3.35 (29.7)	2110 (2.83)	70.0 (158)
3.4.4	11120 (2500)	8000	569 (825)	60.0 (140)	4.48 (7.10)	3.12 (1.23)	6.08 (53.9)	5100 (6.84)	75.6 (168)
4.1.0	4448 (1000)	0	1010 (1465)	55.6 (132)	5.59 (8.81)	6.63 (2.61)	- -	- -	60.6 (141)
4.1.1	4448 (1000)	2000	1010 (1465)	55.6 (132)	5.60 (8.87)	6.50 (2.56)	- -	- -	61.7 (143)
4.1.2	4448 (1000)	4000	1010 (1465)	56.7 (134)	5.64 (8.95)	6.12 (2.41)	0.15 (1.30)	59 (0.08)	65.0 (149)
4.1.3	4448 (1000)	6000	972 (1410)	57.8 (136)	5.68 (9.00)	5.82 (2.29)	4.26 (37.7)	2680 (3.59)	67.8 (154)
4.1.4	4448 (1000)	8000	917 (1330)	57.8 (136)	5.72 (9.07)	5.90 (1.93)	5.78 (51.2)	4850 (6.50)	72.2 (162)
4.2.0	8896 (2000)	0	1010 (1465)	57.8 (136)	5.62 (8.90)	4.72 (1.86)	- -	- -	62.2 (144)
4.2.1	8896 (2000)	2000	1010 (1465)	54.4 (130)	5.60 (8.87)	4.42 (1.74)	- -	- -	61.1 (142)
4.2.2	8896 (2000)	4000	1010 (1465)	55.0 (131)	5.62 (8.91)	4.80 (1.89)	1.36 (12.1)	585 (0.77)	62.2 (144)
4.2.3	8896 (2000)	6000	979 (1420)	56.7 (134)	5.65 (8.95)	4.19 (1.65)	4.26 (37.7)	2680 (3.59)	66.7 (152)
4.2.4	8896 (2000)	8000	924 (1340)	58.9 (138)	5.72 (9.06)	3.84 (1.51)	6.39 (56.6)	5360 (7.18)	72.8 (163)
4.3.0	13344 (3000)	0	1010 (1465)	55.6 (132)	5.46 (8.65)	3.91 (1.54)	- -	- -	61.1 (142)
4.3.1	13344 (3000)	2000	1010 (1465)	54.4 (130)	5.52 (8.75)	3.76 (1.48)	- -	- -	60.0 (140)
4.3.2	13344 (3000)	4000	1010 (1465)	54.4 (130)	5.55 (8.80)	3.89 (1.53)	1.37 (12.1)	585 (0.77)	62.8 (145)
4.3.3	13344 (3000)	6000	979 (1420)	56.1 (133)	5.60 (8.88)	3.66 (1.44)	4.26 (37.7)	2680 (3.59)	67.8 (154)
4.3.4	13344 (3000)	8000	924 (1340)	58.9 (138)	5.63 (8.92)	3.68 (1.45)	7.00 (62.0)	5880 (7.87)	74.4 (166)
4.4.0	17792 (4000)	0	1010 (1465)	56.7 (134)	5.17 (8.20)	3.58 (1.41)	- -	- -	62.2 (144)
4.4.1	17792 (4000)	2000	1010 (1465)	54.4 (130)	5.27 (8.35)	3.22 (1.27)	- -	- -	61.1 (142)
4.4.2	17792 (4000)	4000	1010 (1465)	54.4 (130)	5.31 (8.42)	3.22 (1.27)	1.37 (12.1)	585 (0.77)	63.3 (146)
4.4.3	17792 (4000)	6000	1010 (1465)	55.6 (132)	5.49 (8.70)	3.02 (1.19)	4.72 (41.8)	2970 (3.98)	68.9 (156)
4.4.4	17792 (4000)	8000	1010 (1465)	61.1 (142)	5.74 (9.10)	3.30 (1.30)	6.89 (61.0)	5760 (7.74)	76.7 (170)

*Data Point 1.0 shows ball bearing deflections.

**Data Point 1.2.0 taken as zero reference.

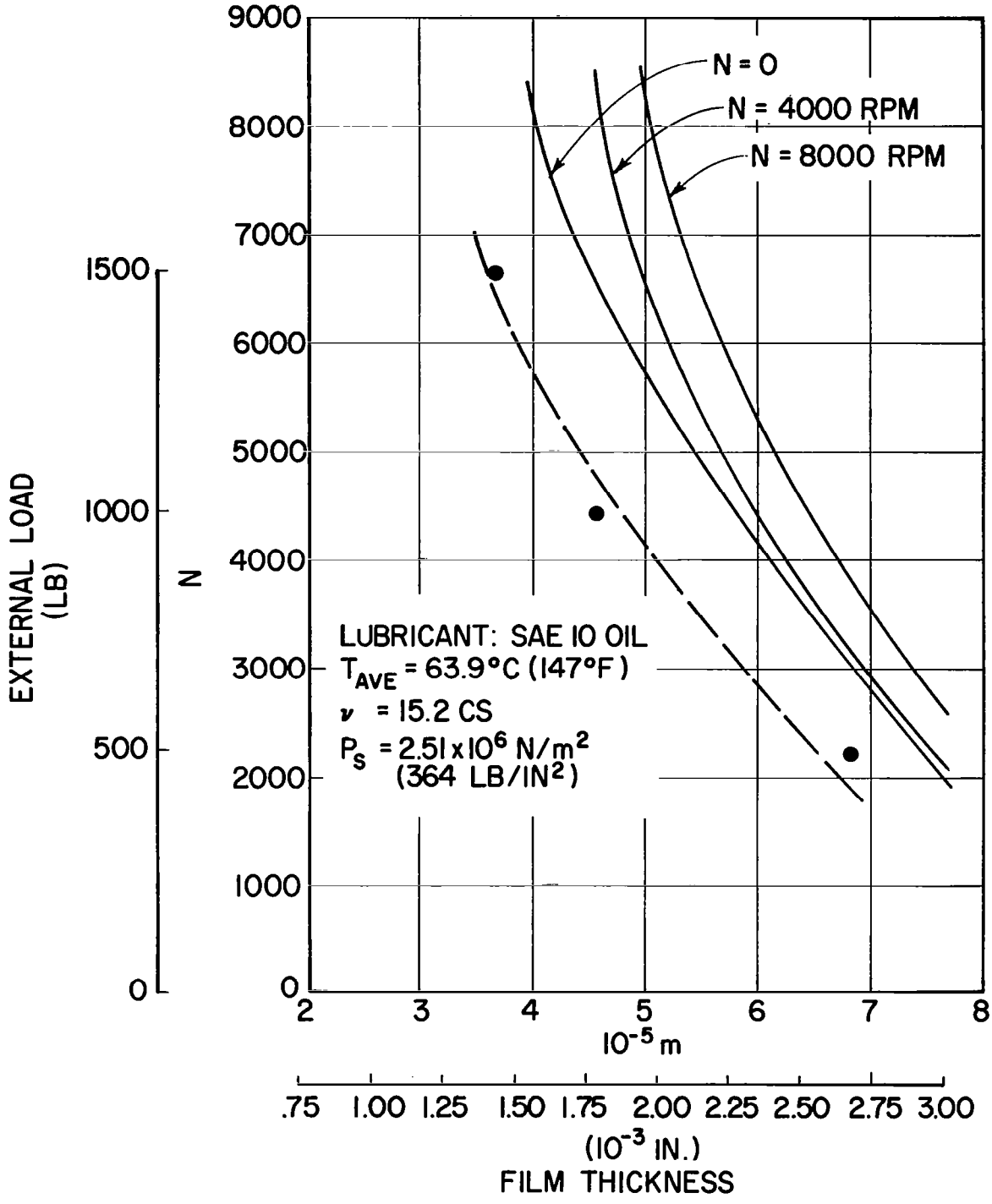

Fig. 13 Load-Deflection Test Results — Fluid Film Bearing Evaluation Lubricant Supply Pressure Equivalent to 10,000 rpm

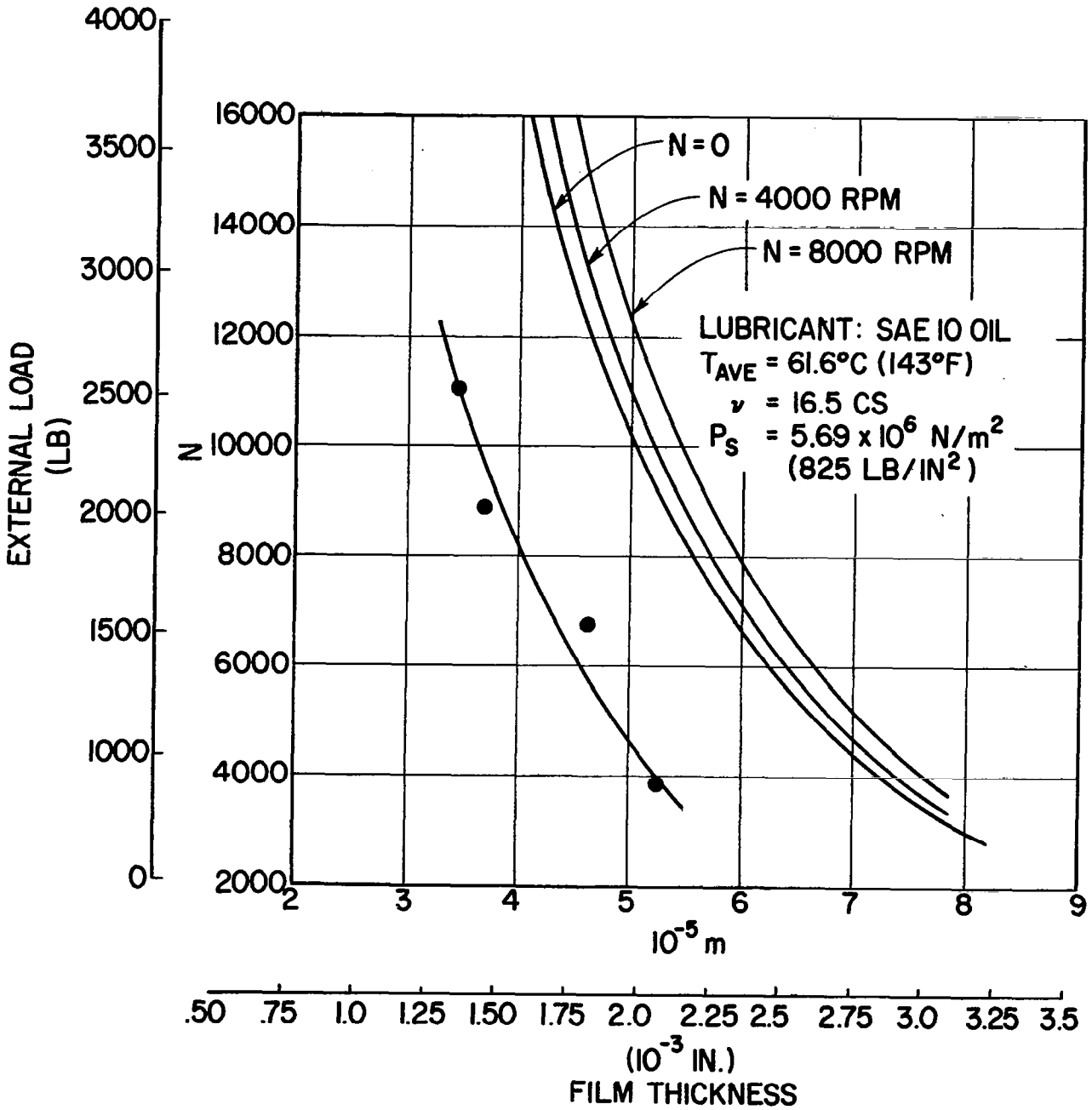

Fig. 14 Load-Deflection Test Results — Fluid Film Bearing Evaluation Lubricant Supply Pressure Equivalent to 15,000 rpm

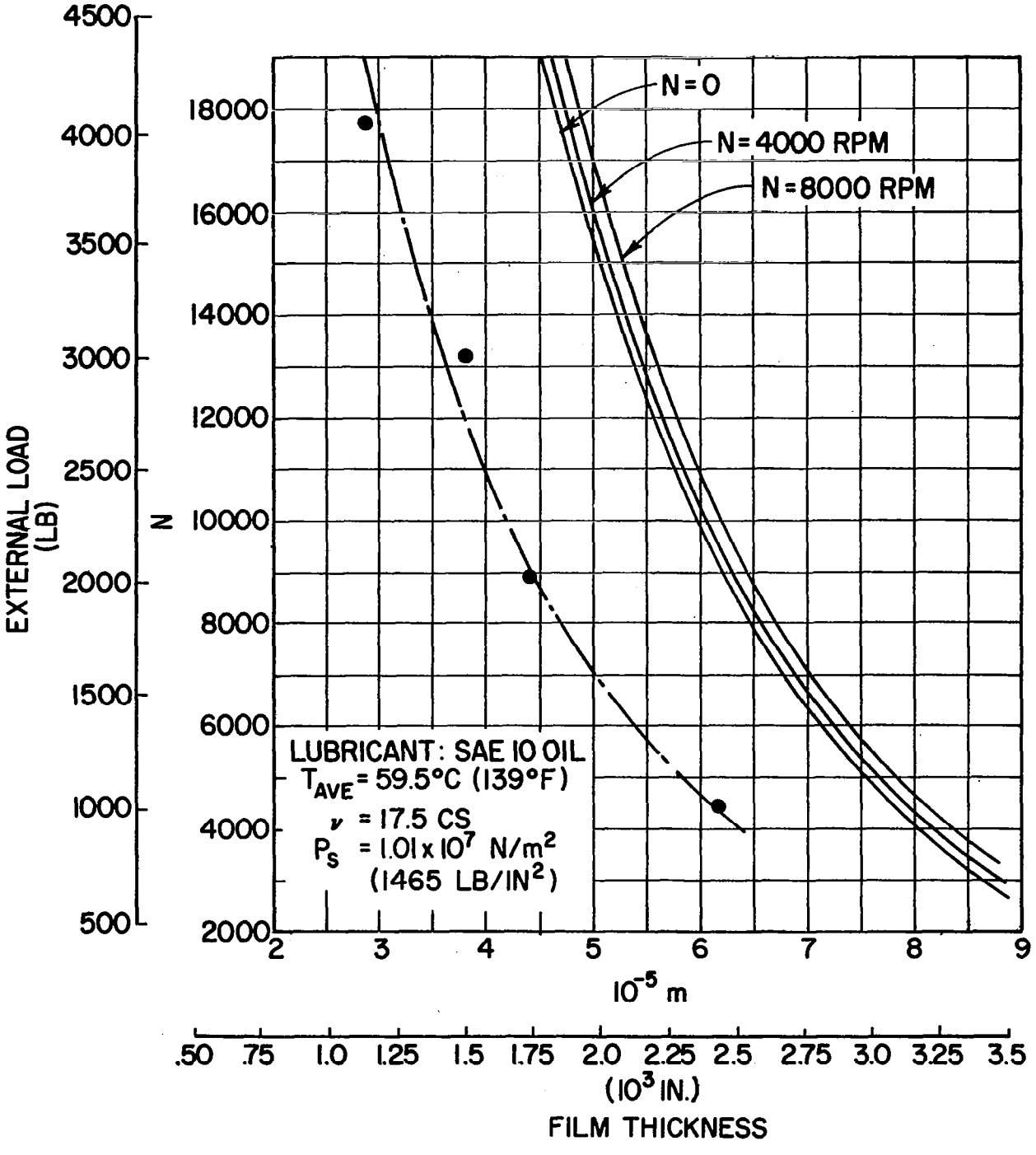

Fig. 15 Load-Deflection Test Results — Fluid Film Bearing Evaluation Lubricant Supply Pressure Equivalent to 20,000 rpm

the bearing stiffness) appears to be in good agreement with predicted trends; however, with reference to Table III for data points 2.0 through 4.0, the measured film thickness usually appears to be decreasing with speed. This phenomenon is in contrast to the normally expected behavior where the increasing speed due to centrifugal augmentation should have raised the load carrying capacity, as shown by the analytical results.

An examination of the film thicknesses listed in Table III indicates that the film thicknesses consistently appear to be 1.27 to 1.91 x 10^{-5} m (0.5 to 0.75 x 10^{-3} in.) lower than the predicted values.

The differences between the experimental measurements and analytically derived film thicknesses can be caused by thermal effects and possible distortions of the fluid-film bearing members not accounted for in the analysis. Discussions of these differences will be presented in more detail in the closing section of this report.

As a result of the thermally induced error effects, the film thickness readings for all speeds were averaged and plotted in terms of average data points disregarding the effect of speed. It should be noted that the speed effect is most pronounced at low supply pressures; at higher supply pressures, the augmenting action of the centrifugal pumping forces represents a smaller fraction of the overall load carrying capacity. For this reason, the error introduced by the averaging of the film thicknesses decreases as the rotational speed of the shaft increases.

The introduction of the sealed oil supply system for the fluid-film bearing permitted exact measurements of its flow requirements. A composite graph indicating the flow rate measurements of the three data points covering the fluid-film bearing test is presented in Figure 16. Superimposed on the test data are analytically derived flow curves based on the actual test conditions. Generally, the agreement between the predicted and calculated values of flow is quite good. The increase in flow rate as speed increases, follows the expected trend (which was not the case with the film thickness data).

Torque measurements taken in conjunction with the flow and film thickness data listed in Table III are grossly understated. The low torque values were obtained mainly because the fluid-film bearing feed system required a large and heavy piping arrangement. When this piping was pressurized to levels as high as 1.1 x $10^7 N/m^2$ (1,465 lb/in^2), it became very stiff and acted as a restraint against the test head rotation required to deflect the torque arms. This restraint which was mainly responsible for the very low torque readings, was practically eliminated in the series hybrid bearing test runs.

In summary, the fluid-film bearing test data indicates ample load carrying capacity at high speeds of operation. According to the obtained test data, loads of 6672 N (1500 lb) can be easily sustained at equivalent DN values of 1.5 million, with flows not exceeding 3.46 x $10^{-4} m^3/sec$ (5.5 gpm). At equivalent DN values of 2.25 million, the load carrying capacity can reach

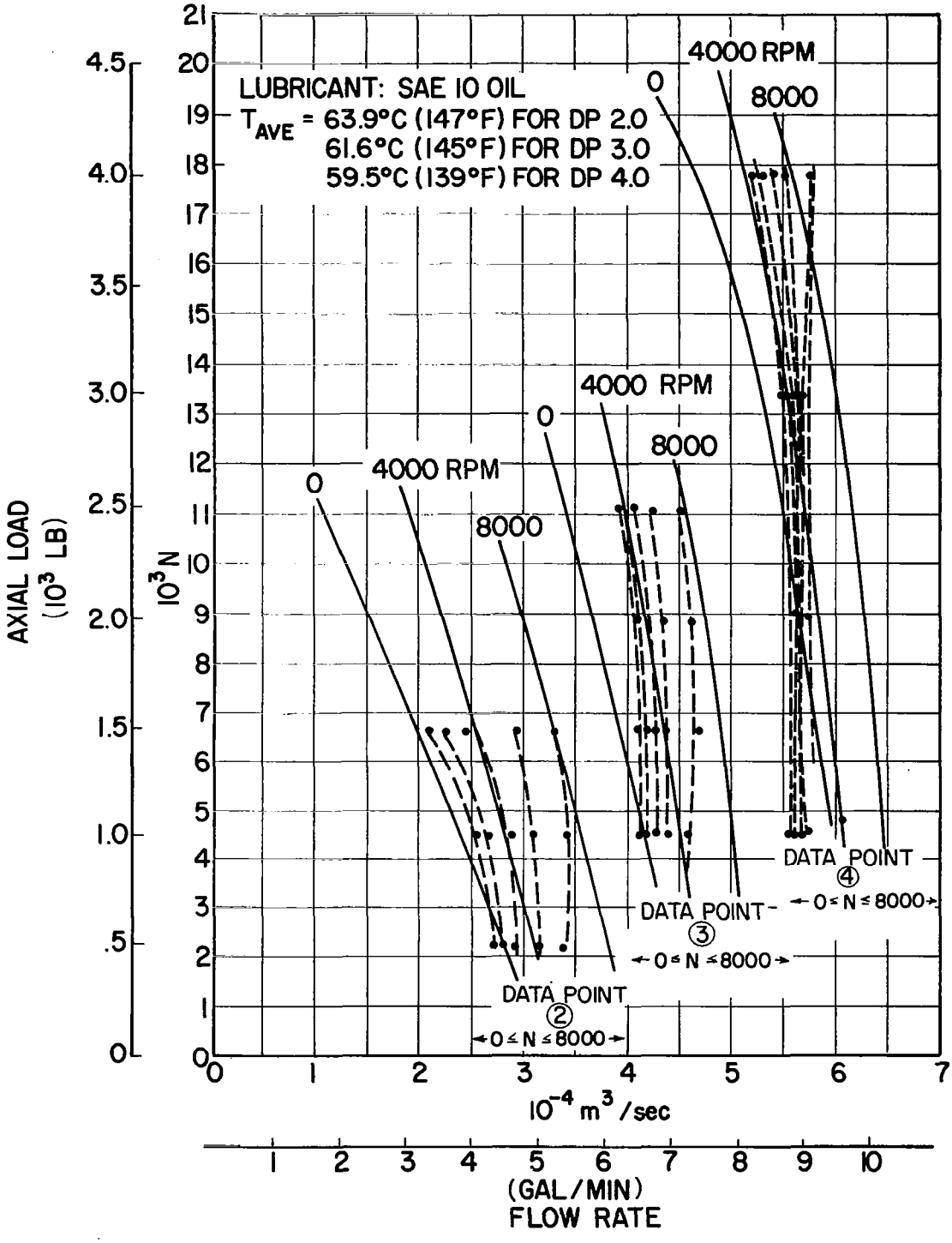

Fig. 16 Flow Rate Measurements — Fluid Film Bearing Evaluation

13,350 N (3000 lb) with the flow not exceeding 4.73 x $10^{-4}m^3$/sec (7.5 gpm) and at an equivalent of 3 million DN, 17,792 N (4000 lb) can be safely supported with flow rates falling below 5.93 x $10^{-4}m^3$/sec (9.5 gpm).

2. Series Hybrid Bearing Tests

The successful completion of the fluid-film bearing tests permitted the restructuring of the test head for initiation of the full hybrid bearing test sequence (Data Point 5.0 on Table II). Two changes in the test set-up were made as part of the restructuring and included a redirecting of the oil supply lines in order to reduce the test head restraint and the deactivation of the ball bearing restraining shear pins. In addition, the test head was thoroughly purged and cleaned of all residual SAE 10 mineral oil and re-plumbed to the MIL-L-23699 oil supply.

Successful tests were conducted on the series hybrid bearing over the speed range of 5000 $\leq$ N $\leq$ 15000 rpm and an axial load range of 4448 N (1000 lb) $\leq$ W $\leq$ 13,344 N (3000 lb). Results of all test data collected are presented in Table IV with the load deflection performance, flow data and torque measurements shown in Figures 17, 18 and 19, respectively.

The film thickness data for the hybrid tests shows the identical behavior pattern as did the data from the fluid-film bearing tests; namely, consistently low values. Examination of the individual probe readings indicates that some misalignment occured as the test conditions were varied, but the apparent low film thickness readings are felt to be primarily caused by the effects noted for the fluid-film bearing test results previously described.

Comparison of both flow and torque data from the hybrid tests with theoretically predicted values indicates excellent correlation, again implying that any discrepancies in the film thickness determination must be a result of either self-compensating thermal effects or by test induced probe zero shifts.

The series hybrid test sequence outlined in Table II was modified slightly during implementation of the test program. It became apparent after the conclusion of Data Point 5.1 that in order to remain within the supply capability of the lubricant pump, higher speed runs would have to be made at higher axial loads. This modification was also necessary to eliminate a possible critical speed problem induced by low fluid-film bearing stiffness. A result of this conclusion was the addition of a 6672 N (1500 lb) and a 8896 N (2000 lb) test to Data Point 5.1 and the substitution of a 13,344 N (3000 lb) for the 4448 N (1000 lb) axial load in Data Point 5.2. A similar approach was tried during the unsuccessful attempt to proceed to Data Point 5.3 (20,000 rpm tests). At the conclusion of the 15,000 rpm, 13,344 N (3000 lb) test point, the load was raised to 15,600 N (3500 lb) and the rotor speed was slowly increased. At a speed very close to 16,500 rpm, the residual pressure supplying the fluid-film bearing reached zero, indicating the lubricant

TABLE IV

HYBRID BEARING PERFORMANCE EXPERIMENTAL RESULTS

Data Point	Axial Load N (lb)	Rotor Speed rpm	Oil Supply Pressure $10^4 N/m^2$ (lb/in^2)	Oil Inlet Temp. °C (°F)	Flow Rate $10^{-4} m^3/sec$ (gpm)	Film Thickness 10^{-5}m(10^{-3}in)	ω_b/ω_s	ω_c/ω_b	Torque N-m(in-lb)	Power Loss Watts (HP)
5.1.1	4448 (1000)	5000	48.3 (70)	93.3 (200)	1.20 (1.9)	2.03 (0.80)	.480	.441	1.46(12.9)	763 (1.02)
5.1.2	4448 (1000)	6000	45.5 (66)	94.4 (202)	1.38 (2.18)	2.11 (0.83)	.470	.450	1.59(14.06)	998 (1.34)
5.1.3	4448 (1000)	7000	41.4 (60)	95.5 (204)	1.60 (2.53)	2.24 (0.88)	.469	.469	2.06(18.28)	1514 (2.03)
5.1.4	4448 (1000)	10000	31.7 (46)	96.6 (206)	2.68 (4.25)	2.74 (1.08)	.483	.478	4.00(35.43)	4194 (5.62)
5.1.5	6672 (1500)	10000	31.0 (45)	96.6 (206)	2.59 (4.10)	2.74 (1.08)	.473	.507	3.18(28.2)	3338 (4.47)
5.1.6	8896 (2000)	10000	35.8 (52)	96.6 (206)	1.78 (2.82)	1.93 (0.76)	.495	.509	3.38(29.95)	3545 (4.75)
5.2.1	8896 (2000)	15000	12.4 (18)	87.8 (190)	3.85 (6.10)	2.26 (0.89)	.475	.577	5.40(47.80)	8487 (11.4)
5.2.2	13344 (3000)	15000	11.7 (17)	82.8 (181)	3.73 (5.92)	0.66 (0.26)	.507	.567	6.03(53.40)	9481 (12.7)
5.2.2.1	13344 (3000)	15000	11.0 (16)	85.5 (186)	3.72 (5.90)	0.56 (0.22)	.507	.612	5.97(52.90)	9392 (12.6)

Data Point	Ball Brg. Outer Race Temp. °C (°F)	Oil Discharge Temp. °C (°F)
5.1.1	98.3 (209)	97.2 (207)
5.1.2	99.4 (211)	98.9 (210)
5.1.3	100 (212)	100 (212)
5.1.4	105 (221)	106 (221)
5.1.5	106 (222)	106 (222)
5.1.6	106 (222)	106 (222)
5.2.1	120 (249)	123 (254)
5.2.2	122 (251)	101 (214)
5.2.2.1	122 (251)	104 (220)

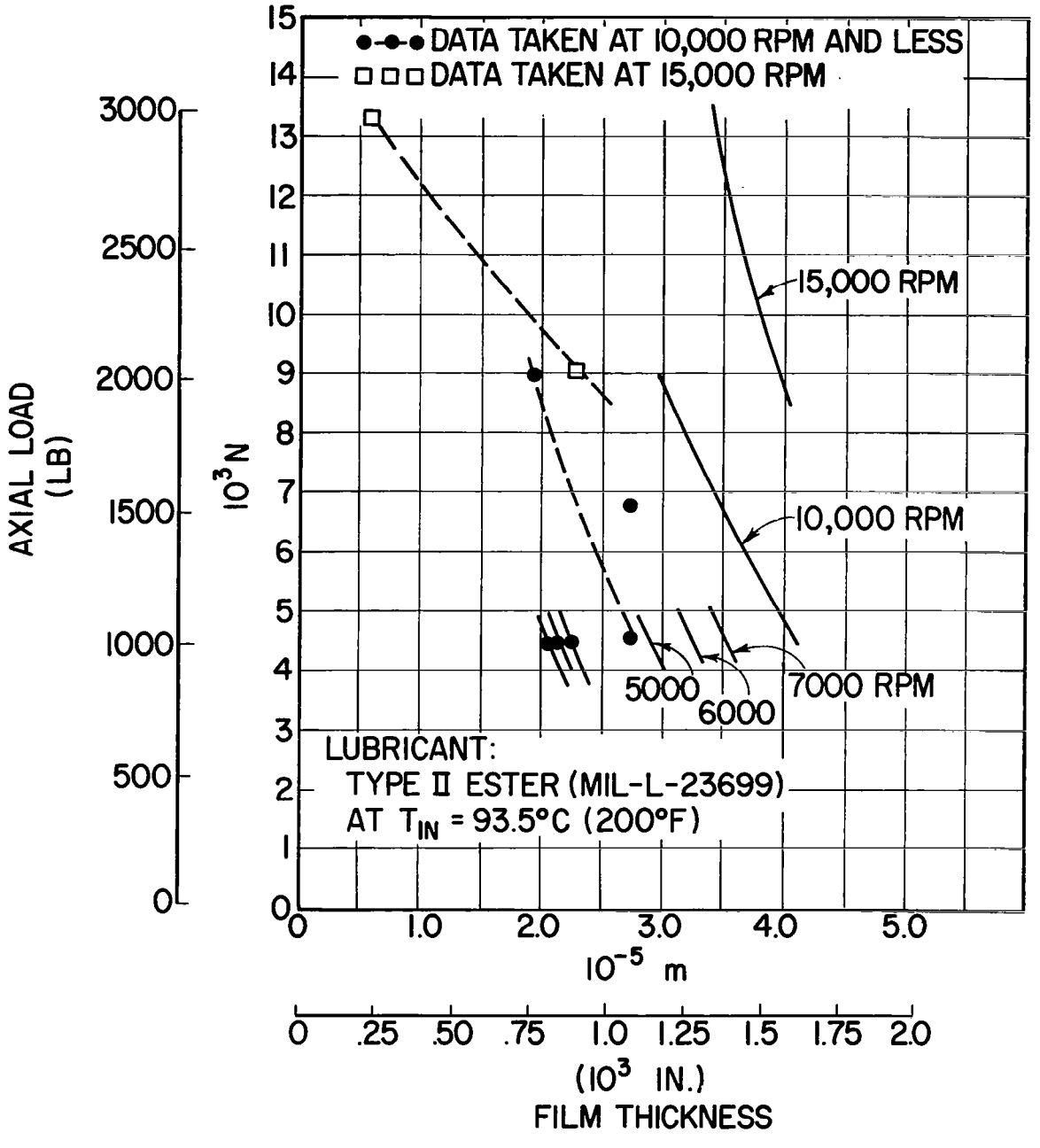

Fig. 17 Load Deflection Test Results — Series Hybrid Bearing

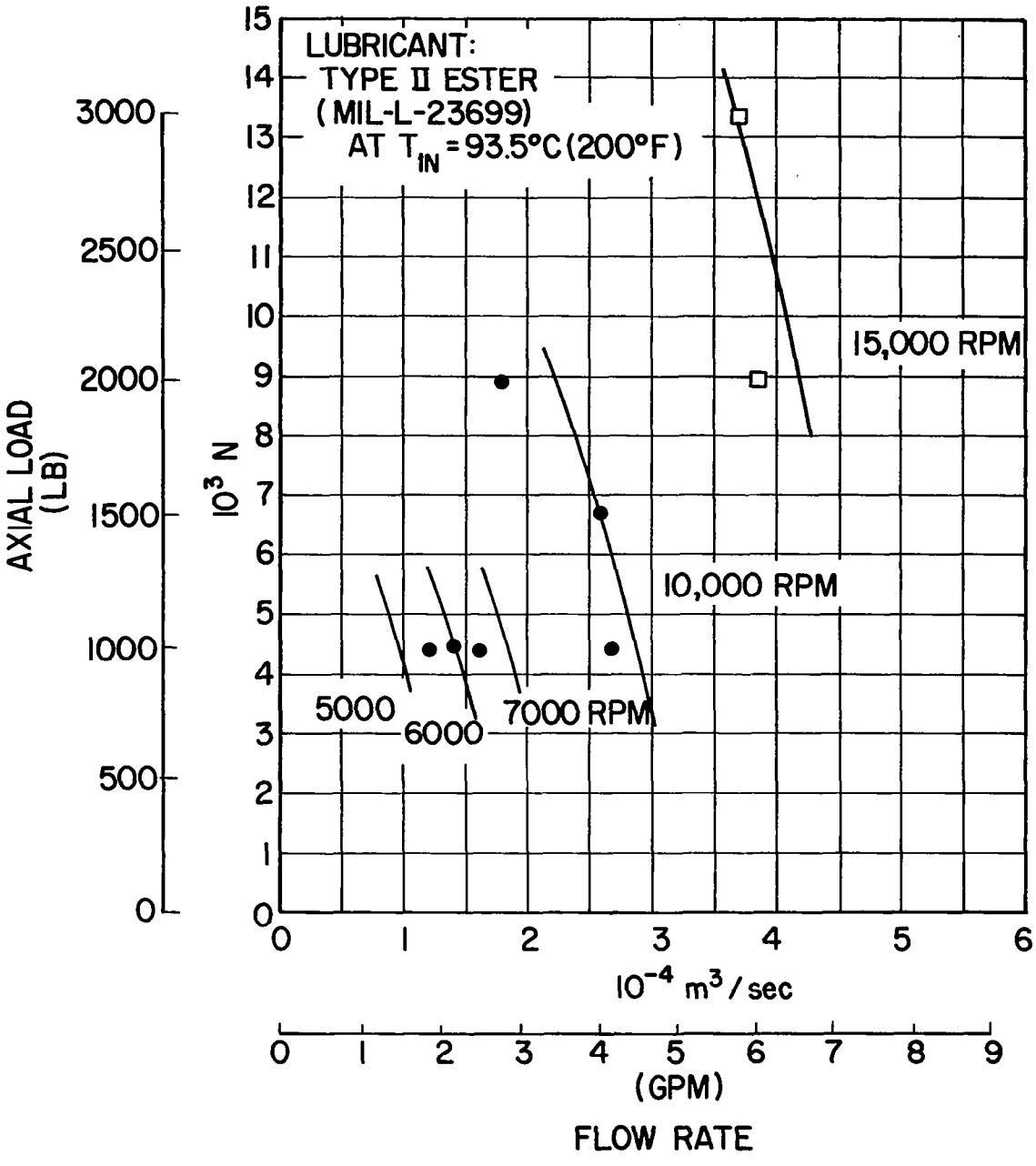

Fig. 18 Flow Rate Measurements — Series Hybrid Bearing

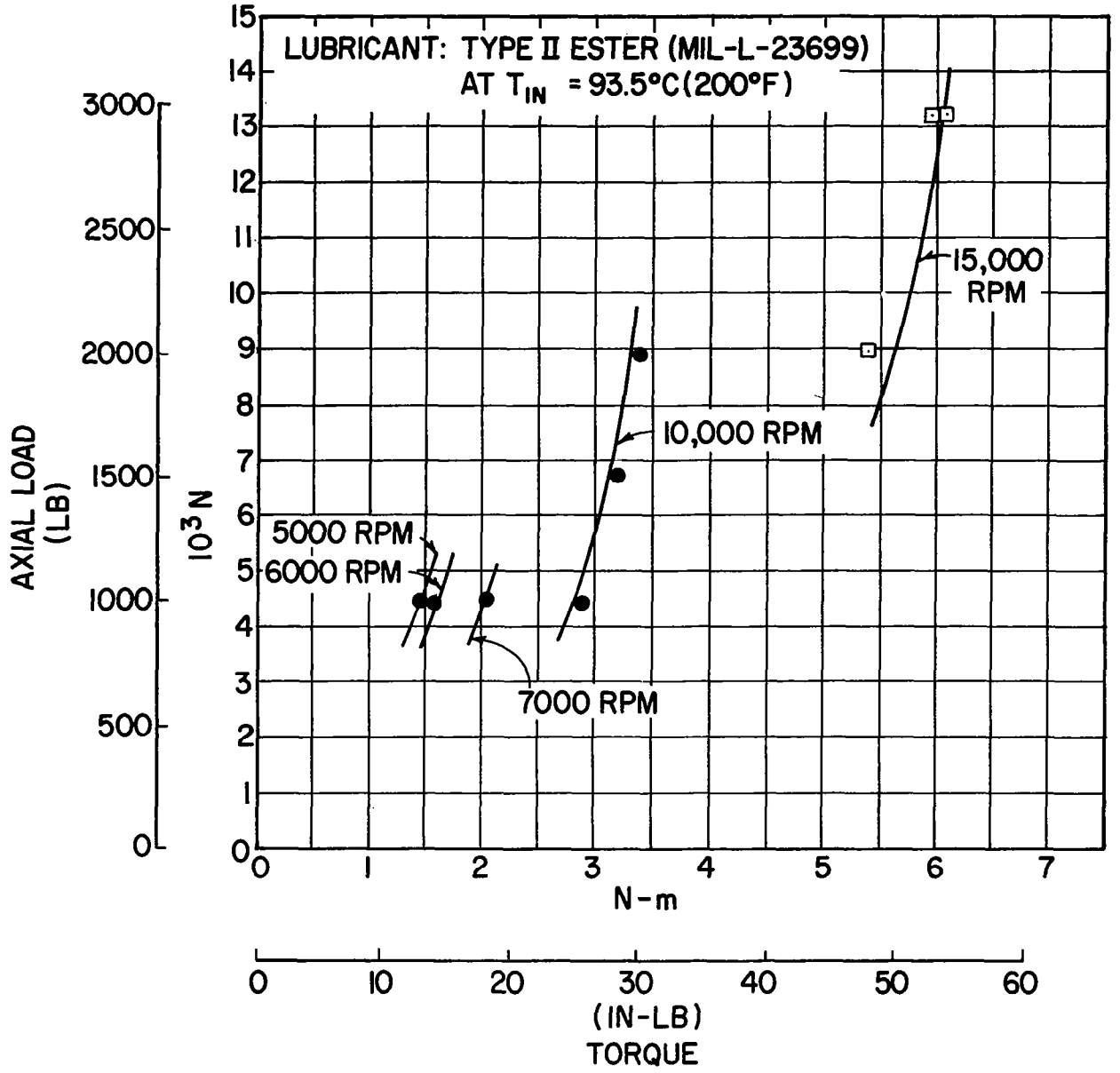

Fig. 19 Torque Measurements — Series Hybrid Bearing

pumping system flow rate maximum had been achieved. The zero supply pressure was considered to be the limiting condition for testing and as a result, the attempt to complete Data Point 5.3 was discontinued.

IV. DISCUSSION OF DEVIATIONS FROM ANALYTICAL PREDICTIONS

Generally, the independent fluid-film bearing tests indicated good performance under all test conditions, but with some anomalies.

Experimentally, it was shown that an increase in rotor speed at constant lubricant supply pressure produces a decrease in the measured bearing clearance. This effect is contrary to the analytical predictions, according to which an increase in speed should produce an increase in film thickness. In addition, the average experimental values of film thickness measured at any individual supply pressure over the test span range, were consistently smaller than the predicted values and always by a nearly similar amount of 1.27×10^{-6} m (5.0×10^{-4} in.).

A plausible explanation for both of the above observed effects, i.e., film thickness reduction with speed, as opposed to analytically demonstrated film thickness increase, and the generally reduced overall measured film thickness level, can lie in the temperature measuring methods employed.

The existing oil temperature (oil leaving the bearing) is measured by thermocouples, attached to the individual probe brackets. The output of these thermocouples is also used to correct for thermal errors inherent in the performance of the proximity probes. These thermocouples are surface mounted with their junction exposed to both the exit oil spray and the metal temperature of the probe holder. Since the probe holder is firmly attached to the housing, the conduction of the heat away from the probe holder will tend to lower the apparent temperature indication of the thermocouple.

Our probe calibration curves generally show a zero shift of about 5.08×10^{-6} meters per °C (1×10^{-4} inches per °F) with no thermal effect on the calibration curve slope. Thus, should the measured temperature reading be off by 2.5°C (5°F), the observed error of 1.27×10^{-6} m (5.0×10^{-4} in.) between the measured and calculated film thickness values could be easily explained. Furthermore, higher relative velocities within the fluid-film bearing, caused by increased rotor speed, will generate higher levels of heat within the bearing clearance, thereby also exaggerating the thermal effect.

The axial thermal gradients resulting from the higher oil film temperatures at the faces of the bearings could also cause thermoelastic deformation which would effectively bring about a distortion of the oil film. Because, however, of the reasonably low temperature increases observed during this test series, it is highly unlikely that the thermal distortions will reach an amplitude significant enough to affect the bearing performance to the indicated degree. It is more likely that the higher than measured temperatures in existence within the oil film (which will bring about a reduction in the oil viscosity) combined with the resulting shift in the probe voltage, are responsible for all the observed deviations between the analytical and test results.

Another apparent discrepancy between the analytically predicted and actual test results concerns the speed division between the ball and fluid-film bearing. Thus, for instance, Figure 13 of Reference 2 predicts ω_b to ω_s ratio of 0.6 for an axial load of 2000 lbs. with the shaft operating at a speed of 15,000 rpm. This means that the ball bearing would be operating at an effective speed of 9,000 rpm. A corresponding point in Table IV (5.2.1) obtained under similar conditions of operation, indicates a ω_b to ω_s ratio of .475 which results in an effective bearing speed of 7,125 rpm. This is an appreciable difference, particularly when one considers the effect of bearing speed on bearing fatigue life.

The speed splits obtained on the tests are obviously more favorable than those originally anticipated by analysis. The split, however, is in a large measure a function of the ball bearing torque. The ball bearing torque values employed in the original analysis were those obtained on test, as reported in Reference 5. These tests were performed with normal ball bearing mounts. In the series hybrid bearing arrangement, the oil emanating from the fluid-film bearing imparts an additional churning torque on the ball bearing inner race or the intermediate member. This will raise the ball bearing torque value and result in a more favorable split. That fact could be utilized to the designer's advantage in future applications, where further reductions in the effective ball bearing speed should be required. In such cases, the intermediate floating member comprised of the outer fluid-film bearing face and the ball bearing inner race, could be designed to impart higher churning losses, and thus result effectively in a ball bearing torque increase which will reduce the effective speed of operation of the ball bearing component. Alternately, additional oil jets could be provided to impinge on the intermediate member and thus slow down its motion.

In most applications, however, it is anticipated that the speed splits obtained in this test set-up will suffice to bring about all the decrease in the effective ball bearing speed required to extend the ball bearing fatigue life to acceptable levels.

NOMENCLATURE

N	Rotational Speed, rpm
P_s	Supply Pressure, N/m^2 (lb/in^2)
T_{ave}	Temperature (Average), °C (°F)
T_{in}	Inlet Temperature, °C (°F)
W	Load, N (lb)
ω_b	Ball Bearing Inner Race Speed, sec^{-1}
ω_c	Ball Bearing Cage Speed, sec^{-1}
ω_s	Shaft Speed, sec^{-1}

REFERENCES

1. Anderson, W. J., Fleming, D. P., and Parker, R. J., "The Series Hybrid Bearing - A New High-Speed Bearing Concept," Transactions of ASME, Vol. 94, Series F, No. 2, April 1972.

2. Gu, A., Eusepi, M. W. and Winn, L. W., "Evaluation of a Series Hybrid Thrust Bearing at DN Values of Three Million," NASA CR-2366, January 1974.

3. Winn, L. W., Badgley, R. H., "Development of Long-Life Jet Engine Thrust Bearings," NASA CR-72744, June 1970.

4. Pan, C.H.T., and Malanoski, S.B., "Analysis of Fluid-Film Thrust Bearings With Allowance for Temperature Dependent Viscosity," NASA CR-2052, May 1972.

5. Scibbe, H. W., Munson, H. E., "Experimental and Predicted Performance of 150 mm Bore Solid and Drilled Ball Bearings To 3 Million DN," NASA TN D-7737.

NASA-Langley, 1975 E-8266